NASA TECHNICAL MEMORANDUM

NASA TM X-53982

WIND DETERMINATION BASED ON EDDY TRANSIT TIMES MEASURED BETWEEN FOUR NON-INTERSECTING LIGHT BEAMS

By W. H. Heybey
Aero-Astrodynamics Laboratory

December 22, 1969

NASA

George C. Marshall Space Flight Center
Marshall Space Flight Center, Alabama

TECHNICAL REPORT STANDARD TITLE PAGE

1. REPORT NO. TM X-53982	2. GOVERNMENT ACCESSION NO.	3. RECIPIENT'S CATALOG NO.
4. TITLE AND SUBTITLE WIND DETERMINATION BASED ON EDDY TRANSIT TIMES MEASURED BETWEEN FOUR NON-INTERSECTING LIGHT BEAMS		5. REPORT DATE December 22, 1969 6. PERFORMING ORGANIZATION CODE
7. AUTHOR(S) W. H. Heybey		8. PERFORMING ORGANIZATION REPORT #
9. PERFORMING ORGANIZATION NAME AND ADDRESS Aero-Astrodynamics Laboratory George C. Marshall Space Flight Center Marshall Space Flight Center, Alabama 35812		10. WORK UNIT NO. 11. CONTRACT OR GRANT NO. 13. TYPE OF REPORT & PERIOD COVERED
12. SPONSORING AGENCY NAME AND ADDRESS		Technical Memorandum 14. SPONSORING AGENCY CODE
15. SUPPLEMENTARY NOTES		

16. ABSTRACT

An atmospheric eddy crossing successively the lines of sight (beams) of two telescopes stays between them for a time that can be discovered through cross correlation of the light intensity variation recorded by the receivers. Three such observed times are needed for determining the motion of the wind that carries the eddies along; they supply the experimental input.

The length and location of the paths vary with the beam arrangement and with the wind vector which, in the present paper, is taken as constant throughout a suitably bounded observation volume. At least four detectors are required for monitoring winds of unknown azimuthal direction. They are conveniently placed at the corners of a square sitting on level ground. Its dimensions and the detector orientation (beam direction) depend in part on observation height, in part on various restraints inherent in the problem, among them the need to hold down the observation volume. These restraints determine the range in which an observed transit time triplet can be trusted to have been generated by one and the same wind, measured accurately enough to warrant the computation of its components from the expressions given for them. The range alters with the beam configuration, as does the height span accessible to the latter. Care has been taken to define configurations capable of detecting winds regardless of lateral direction. Owing to restraints, however, allowable wind inclination then remains within bounds.

17. KEY WORDS	18. DISTRIBUTION STATEMENT PUBLIC RELEASE: E. D. Geissler E. D. Geissler Director, Aero-Astrodynamics Laboratory

19. SECURITY CLASSIF. (of this report)	20. SECURITY CLASSIF. (of this page)	21. NO. OF PAGES	22. PRICE
UNCLASSIFIED	UNCLASSIFIED	70	

MSFC - Form 3292 (May 1969)

TABLE OF CONTENTS

TECHNICAL MEMORANDUM X-53982

WIND DETERMINATION BASED ON EDDY TRANSIT TIMES MEASURED BETWEEN FOUR NON-INTERSECTING LIGHT BEAMS

SUMMARY

The problem and the conditions imposed on it are identified in an introductory section. To observe winds from whichever compass point they may arrive, a symmetric arrangement of four beams is introduced. It contains three free geometric parameters and offers 20 transit combinations of three each, among which 16 can be employed for wind determination. Twelve of them are put to actual use. They are divided into groups of four, each of which is capable of detecting a certain class of winds subject to prescribed terms of confidence and accuracy. Class limits depend on two transit time ratios and take the form of curves bounding off areas within which those ratios may be said to refer to an observable uniform wind blowing in a definite spatial region. With a suitably constructed beam system, it may have any lateral direction. Allowable wind inclinations vary with azimuth and the values adopted for the three geometric and some interrelated parameters reflecting physical and other restraints under which the system is to operate. Many of the accessible winds are measured more than once by the three groups taken together.

The class (or admissibility) areas can be delineated without deciding on the reference or observation height near which one may wish to explore the air motion. However, being linked to parameters used, it cannot be chosen completely at will. With the beam arrangement developed and studied in the main body of the paper, upward and downward winds with inclinations running from 0 to well over 30 degrees are accessible to measurement, provided they move at reference heights roughly between 25 and 300 meters. The location and dimensions of the observation volume can be determined as well.

Homologous systems arising by the same general method when applied to different sets of parameters are capable of observation at lower and greater heights. The calculation of the then measurable wind inclinations is bound up with that of the admissibility areas which is laborious and has not been carried out.

I. INTRODUCTION

To provide for the measurement of winds irrespective of direction and slant angle is recognized as a major concern of crossed-beam atmospheric experimentation (which substitutes the eddy or (mass) convection speed for that of the wind). The instrumentation and data processing phases are pursued elsewhere and need not be considered here. The present report acknowledges the end product of the experimental chain, namely, a number of eddy transit times, and asks the question: What wind produced it? Evidently, these figures vary with the beam configuration operative which, however, is not entirely at our discretion. It must be shaped to answer certain requirements necessary to insure trustworthy measurement.

The most pressing need is to keep the beams close together in the region selected for observation, so that the air flow there can be considered uniform with straight cylindrical eddy paths representing its direction. Their cross sections ought to be comparable to beam width, preferably smaller than it. The volume of the region will be compact as desired if the beam connections established by any and all eddy motions that may occur in it are not too far apart to invalidate the assumption of uniform flow. This sweeping requirement, however, cannot be sustained, except perhaps if a large number of detectors can be brought into action. Practically, one is led to define a class of measurable winds. No restriction as to azimuths will be placed on them in the present investigation. Since nearly horizontal winds, as the most common kind, ought to be detectable at any rate, it is the elevation angle that will be subject to an upper bound beyond which safe measurement is precluded on the ground that over large cross distances the wind vector cannot be expected to stay reasonably constant. To a lesser degree this is also true in the lengthwise direction; however, the restriction thus suggested on path length receives added force by the desire to keep the traveling eddy from decay which would destroy the root of the method. The path length restriction may sometimes be violated when the cross distances are still sufficiently small and then is dominant in limiting the class of observable winds.

The experimental error is assumed not to exceed ±0.1 second. Different ideas can, of course, be put forth on this head which will alter the distribution of safely measurable winds. They will not affect, however, the general reasoning followed in the paper. The transmitted errors vary in inverse proportion to the eddy sojourn time in between beams so that, in order to keep them reasonably small, a lower limit will have to be placed on transit times. If it is put at one second, an observational error of not more than 10 percent is held permissible. As a corollary, no path available to eddy travel must have a shorter length than the strongest admitted wind would cover in unit time. (To be sure, this would not exclude even stronger winds if they happened to blow in the directions of longer beam connections.) The need for maintaining a minimum path length might prevail over the need for short cross distances and then curtail the class of accessible winds in its stead.

Outside the observation region, the wind may shift direction thus giving rise to the recording of extraneous travel times that must not be used for determining a wind vector. Such "forbidden" times can as a rule be recognized by assembling all those that are consonant with transitions available within the monitored volume. An outside transition would require a time either too long or too short except in rare cases where the wind, besides shifting, simultaneously alters its strength within a definite narrow compass. To establish an "admissibility" roster is a major concern of the investigation.

Sometimes spurious transits originating through what may be lumped together as noise effects may be eliminated by the same criterion. However, since the times by which they are indicated do not arise from beam geometry, they may on occasion be found among those admissible. Independent rules for weeding them out are desirable. One at least has already been propounded on a statistical basis.

It is evident from the foregoing that several options have to be exercised before arriving at the final figures for a beam configuration. The numerical decisions made in the paper at certain crucial stations of the development are not immutable. The arrangement described is but one of many that are similar (or even dissimilar if the stress is on different classes of winds).

For ease of the mathematical formulation the beams and eddy paths in what follows are replaced by their center lines. The outer reaches of the admissibility region appear clearly marked off as a consequence, whereas in physical reality the border is not quite so sharply defined.

II. BASIC CONSIDERATIONS

Observation of the three-dimensional wind vector requires a minimum of three beams. Such a configuration has been studied in reference 1,* where an arrangement best suitable for measuring horizontal winds arriving from a 90-degree azimuthal compass has been obtained. The mathematical foundation was couched in general terms, so that an array of non-horizontal winds accessible to measurement by the same arrangement could also have been determined. It is tempting to use it as a base and, by adding a fourth beam, to seek to widen the observational range to

---

*W. H. Heybey, Wind vector calculation using crossed-beam data and detector arrangement for horizontal winds, NASA TM X-53754, July 11, 1968.

include winds from all directions. This line of approach, however, has met with failure, as one might have anticipated. An arrangement more symmetric than any one connected with that of reference 1 is more likely to reach the goal.

Let us introduce a right-handed rectangular Cartesian system with the x- and y-axes on level ground, pointing forward and to the right, respectively. The most symmetric layout of four detectors would place them on these axes, each at the same distance, s, undetermined as yet, from the origin. Their positions then are

$$\begin{cases} 1^{st} \text{ detector (beam a): at } P_a(x_a = s,\ y_a = 0,\ z_a = 0) \\ 2^{nd} \text{ detector (beam b): at } P_b\ (0,s,0) \\ 3^{rd} \text{ detector (beam c): at } P_c\ (-s,0,0) \\ 4^{th} \text{ detector (beam d): at } P_d\ (0,-s,0). \end{cases} \qquad (1)$$

The detectors are sitting at the corners of a square of diagonal length 2s.

In order to define a symmetrical beam system let us introduce a parallel, smaller square whose center is on the z-axis at the "reference" height z = h. Using a positive dimensionless parameter

$$0 < \lambda \leqq 1$$

we may write the coordinates of its corner points as

$$P'_a(0,\lambda s,h),\ P'_b(-\lambda s,0,h),\ P'_c(0,-\lambda s,h),\ P'_d(\lambda s,0,h).$$

The beams a, b, c, d will then be fixed by the segments

$$P_aP'_a,\quad P_bP'_b,\quad P_cP'_c,\quad P_dP'_d,$$

respectively. Note that if λ were to be larger than unity they would diverge, rendering it impossible to bring them close together near any positive reference or "observation" height. Their direction cosines are found as

$$\begin{cases} \alpha_1 = -\sigma\alpha_3, & \alpha_2 = \lambda\sigma\alpha_3, & \alpha_3 = \sin\psi \\ \beta_1 = -\lambda\sigma\alpha_3, & \beta_2 = -\sigma\alpha_3, & \beta_3 = \alpha_3 \\ \gamma_1 = \sigma\alpha_3, & \gamma_2 = -\lambda\sigma\alpha_3, & \gamma_3 = \alpha_3 \\ \delta_1 = \lambda\sigma\alpha_3, & \delta_2 = \sigma\alpha_3, & \delta_3 = \alpha_3 \end{cases} \tag{2}$$

where

$$\sigma = s/h, \qquad \operatorname{cotg}\psi = \sigma\sqrt{1 + \lambda^2}. \tag{3}$$

The acute angle ψ is the elevation angle common to the four beams and so far a free parameter.

Figure 1 shows the top view of the configuration, while Figure 2 offers a look into the first octant of the Cartesian system.

In reference 1 no beforehand decisions were made either on detector positions or on beam directions. Much of the flexibility granted thereby and put to good use is lost with the present arrangement. However, this lack in freedom is not really serious, largely on the grounds that now six transitions are available (instead of three, composing one single transit triad). Selecting suitable connection line triplets out of the $\binom{6}{3} = 20$ that are conceivable with four beams, in fact, makes up for the relative rigidity of the geometry, in which are now only three free parameters (s,h,λ). It will later be seen that their values can be adjusted such that winds arriving from a surprisingly large azimuthal sector can be handled by every transit combination employed, although with horizontal winds, none of them is capable of monitoring a 90-degree compass by itself, as is the single triad of reference 1. We will have to be content with smaller sectors, which, however, must be wide enough to cause the azimuthal reaches of the pertinent triads to overlap. Taken together, they must cover the entire rose in order to achieve a prime objective of the investigation.

Not all of the twenty transit groups of three each will actually be used. Among those that are, the built-in symmetry relations greatly reduce the mathematical labor involved in their study. Nevertheless, before symmetry properties can be invoked, some lengthy formulations are unavoidable in dealing with four beams and six beam connections.

III. POSITION VECTORS, EDDY PATHS, RESTRAINING PLANES

The location of the points P_a ... P_d may be described by their position vectors

$$\underline{r}_a = \underline{i}s, \quad \underline{r}_b = \underline{j}s, \quad \underline{r}_c = -\underline{i}s, \quad \underline{r}_d = -\underline{j}s, \tag{4}$$

where $\underline{i}$, $\underline{j}$, $\underline{k}$ are the unit vectors on the coordinate axes.

Of much greater importance are those particular points on the beams whose connections are parallel to the unknown wind vector

$$\underline{V} = \underline{i}V_1 + \underline{j}V_2 + \underline{k}V_3. \tag{5}$$

It has been shown in reference 1 that for any wind direction there exists exactly one such connection between two beams.* Thus, wind direction alone uniquely defines the terminals of a connecting line whose length, if divided by the measured transit time, yields the wind speed. As another consequence, the analytic expressions for the terminals position vectors are not dependent on wind speed; rather, they contain the ratios of the wind vector components, and, in fact, are linear homogeneous functions of them as given in reference 1, p. 13. For needed clarity the number indices used there will be replaced here by letter indices ($\underline{r}_1 \rightarrow \underline{r}_a$, $\underline{r}_1^* \rightarrow \underline{r}_{ab}^*$, $\underline{r}_2 \rightarrow \underline{r}_b$, $r_2^* \rightarrow \underline{r}_{ba}^*$, etc.). With double-letter subscripts the first letter denotes the beam the terminal sits on, the second indicates to which beam the wind vector drawn through it is pointing. Evaluation of the expressions in terms of the detector coordinates (1) and the direction cosines (2) yields a group of formulas:

$$\underline{r}_{ab}^* = \underline{r}_a + \frac{h}{\alpha_3}\,\underline{\alpha}\,\frac{V_1 + V_2 + V_3\sigma(1+\lambda)}{V_1(1+\lambda) + V_2(1-\lambda) + V_3\sigma(1+\lambda^2)}$$

(equations (6) continued on next page)

*When the wind happens to be parallel to the parallel planes in which they are contained, there exists none. Such winds must and can be handled by other beam pairs.

$$
\begin{aligned}
\underline{r}^*_{ba} &= \underline{r}_b + \frac{h}{\alpha_3}\underline{\beta}\frac{V_1 + V_2 + V_3\sigma(1-\lambda)}{V_1(1+\lambda) + V_2(1-\lambda) + V_3\sigma(1+\lambda^2)} \\
\underline{r}^*_{bc} &= \underline{r}_b + \frac{h}{\alpha_3}\underline{\beta}\frac{V_1 - V_2 - V_3\sigma(1+\lambda)}{V_1(1-\lambda) - V_2(1+\lambda) - V_3\sigma(1+\lambda^2)} \\
\underline{r}^*_{cb} &= \underline{r}_c + \frac{h}{\alpha_3}\underline{\chi}\frac{V_1 - V_2 - V_3\sigma(1-\lambda)}{V_1(1-\lambda) - V_2(1+\lambda) - V_3\sigma(1+\lambda^2)} \\
\underline{r}^*_{cd} &= \underline{r}_c + \frac{h}{\alpha_3}\underline{\chi}\frac{V_1 + V_2 - V_3\sigma(1+\lambda)}{V_1(1+\lambda) + V_2(1-\lambda) - V_3\sigma(1+\lambda^2)} \\
\underline{r}^*_{dc} &= \underline{r}_d + \frac{h}{\alpha_3}\underline{\delta}\frac{V_1 + V_2 - V_3\sigma(1-\lambda)}{V_1(1+\lambda) + V_2(1-\lambda) - V_3\sigma(1+\lambda^2)} \\
\underline{r}^*_{da} &= \underline{r}_d + \frac{h}{\alpha_3}\underline{\delta}\frac{V_1 - V_2 + V_3\sigma(1+\lambda)}{V_1(1-\lambda) - V_2(1+\lambda) + V_3\sigma(1+\lambda^2)} \\
\underline{r}^*_{ad} &= \underline{r}_a + \frac{h}{\alpha_3}\underline{\alpha}\frac{V_1 - V_2 + V_3\sigma(1-\lambda)}{V_1(1-\lambda) - V_2(1+\lambda) + V_3\sigma(1+\lambda^2)} \\
\underline{r}^*_{ac} &= \underline{r}_a + \frac{h}{\alpha_3}\underline{\alpha}\frac{V_2 + \lambda\sigma V_3}{\lambda V_1 + V_2} \\
\underline{r}^*_{ca} &= \underline{r}_c + \frac{h}{\alpha_3}\underline{\chi}\frac{V_2 - \lambda\sigma V_3}{\lambda V_1 + V_2} \\
\underline{r}^*_{bd} &= \underline{r}_b + \frac{h}{\alpha_3}\underline{\beta}\frac{V_1 - \lambda\sigma V_3}{V_1 - \lambda V_2} \\
\underline{r}^*_{db} &= \underline{r}_d + \frac{h}{\alpha_3}\underline{\delta}\frac{V_1 + \lambda\sigma V_3}{V_1 - \lambda V_2} .
\end{aligned}
\tag{6}
$$

The unit vector components v_i appearing in reference 1 have been replaced here by the wind vector components $V_i = v_i V$ themselves. Furthermore, $\underline{\alpha}$, $\underline{\beta}$, $\underline{\chi}$, $\underline{\delta}$ are the unit vectors in beam direction

($\underline{\alpha} = \alpha_1\underline{i} + \alpha_2\underline{j} + \alpha_3\underline{k}$, etc.). Since $\alpha_3 = \beta_3 = \gamma_3 = \delta_3$, the z-components of two vectors with interchanged index sequence are seen to be equal when $V_3 = 0$, as is geometrically evident with horizontal transits. Four

The group (6) can be considered a main result. All things essential can be derived from it, as indeed it embodies the geometric core of the problem in that, from among the multitude of eddy courses present in a given uniform wind motion, it singles out the six to which a meaningful path length and therefore a measured transit time can be ascribed.

The directed lengths of the several paths may be written as

$$\underline{R}^*_{ab} \equiv \underline{r}^*_{ba} - \underline{r}^*_{ab} = -2\lambda s \frac{\underline{V}}{V_1(1+\lambda) + V_2(1-\lambda) + V_3\sigma(1+\lambda^2)}$$

$$\underline{R}^*_{bc} = \underline{r}^*_{cb} - \underline{r}^*_{bc} = 2\lambda s \frac{\underline{V}}{V_1(1-\lambda) - V_2(1+\lambda) - V_3\sigma(1+\lambda^2)}$$

$$\underline{R}^*_{cd} = \underline{r}^*_{dc} - \underline{r}^*_{cd} = 2\lambda s \frac{\underline{V}}{V_1(1+\lambda) + V_2(1-\lambda) - V_3\sigma(1+\lambda^2)} \qquad (7)$$

$$\underline{R}^*_{da} = \underline{r}^*_{ad} - \underline{r}^*_{da} = -2\lambda s \frac{\underline{V}}{V_1(1-\lambda) - V_2(1+\lambda) + V_3\sigma(1+\lambda^2)}$$

$$\underline{R}^*_{ac} = \underline{r}^*_{ca} - \underline{r}^*_{ac} = -2\lambda s \frac{\underline{V}}{\lambda V_1 + V_2}$$

$$\underline{R}^*_{bd} = \underline{r}^*_{db} - \underline{r}^*_{bd} = 2\lambda s \frac{\underline{V}}{V_1 - \lambda V_2} .$$

These expressions are gained by combined use of relations (2) through (6). The path length vector, $\underline{R}^*_{mn}$, connecting beam m and n (in that order) is either parallel or antiparallel to $\underline{V}$, depending on whether the coefficient at right is positive or negative. This distinction affects the sign of the transit time. If the uniform flow relationship is written as

$$\underline{R}^*_{mn} = \tau^*_{mn} \underline{V} \qquad (8)$$

the transit time τ^*_{mn} is defined as positive or negative with eddies moving from beam m to beam n, or oppositely so, in which case $\tau^*_{mn} = -\tau^*_{nm} < 0$. As a practical consequence, one must, in correlating, delay record n versus record m ($\tau^*_{mn} > 0$) as well as vice versa ($\tau^*_{mn} < 0$), since of course the direction of the flow is unknown.

Eddy travel between separated beams requires a finite time, so that record correlation can never exhibit a peak at time $\tau^*_{mn} = 0$. Should such a peak arise nevertheless, one would first try to put its presence down to extraneous circumstances and simply discard it. If this is not warranted by a noise peak criterion, its occurrence may suggest inadequate operation or undesirable flow properties (as over-sized eddies or winds too strong); the validity of any other maximum is likewise dubious in such cases.

Ideally, in each correlation curve, there is just one relevant peak defining one single transit time.* If, after removing the noise peaks, we are still left with several "wind" peaks, all but one of them will have been caused by shifted winds outside the observation region. The admissibility roster will point out the "true" peak. If even after consulting it, a multiple choice persists, the measurement will have to be abandoned as ambiguous. In anticipating later results it may be added here that, fortunately, many winds can be observed by more than one transit triad, not all of which may use the pair with the inconclusive correlation pattern.

Relations (7) and (8) establish the dependence of the wind vector components present on the travel times registered and thereby furnish the basis for answering the paper's main problem as it was formulated in the Introduction. After calculating the three components, the lateral direction of the wind is found from

$$\tan \varphi = \frac{V_2}{V_1} \tag{9}$$

where the azimuthal angle φ is counted counterclockwise from the positive x-axis. The signs of V_1 and V_2 indicate which one of the two supplementary directions must be assigned to the wind. Its elevation angle is defined by

$$\tan \chi = \frac{V_3}{\sqrt{V_1^2 + V_2^2}} \tag{10}$$

---

*Occasionally there is none (in the circumstances mentioned in the preceding footnote). Any particular beam pair (m,n) is unfit for detecting certain winds.

where the root will be taken absolutely, so that the angle χ is acute or obtuse depending on whether the air is moving upward or downward.

On account of the symmetric beam configuration, the six parallel connecting paths associated with a uniform wind ought to have interrelated lengths, so that the eddy travel times cannot be expected to be wholly independent of each other. Combining the expressions (7) and (8) one can indeed show that, for any wind whatsoever, the relations exist

$$\frac{1}{\tau^*_{ab}} + \frac{1}{\tau^*_{cd}} = \frac{1}{\tau^*_{bc}} + \frac{1}{\tau^*_{da}}$$

$$\frac{2}{\tau^*_{ac}} = \frac{1}{\tau^*_{ab}} - \frac{1}{\tau^*_{da}} \tag{11}$$

$$\frac{2}{\tau^*_{bd}} = \frac{1}{\tau^*_{cd}} - \frac{1}{\tau^*_{da}} .$$

If three travel times are known, the remaining three can be computed from the system (11) which therefore could be used to check the results obtained through back-and-forth correlation of the six record pairs. Approximately, equations (11) ought to be satisfied and thus may serve to remove unrelated correlation peaks, especially if the admissibility roster leaves doubt in this respect.

Since the velocity components can be expressed in terms of transit times, the equality (8) converts path length restrictions into conditions which pronounce certain time sets as inadmissible and, as was mentioned earlier, sometimes take precedence over the limitations imposed by the physical necessity of restraining what had loosely been called the cross distances of the eddy paths.

To fix ideas here consider an inclined straight streamline and the vertical plane in which it is contained. In the operation region one may presume the wind reasonably constant in lateral directions, more precisely, in a plane, E, that passes through a given connecting path and is perpendicular to the vertical plane. Wind shear will sooner be expected in the direction of the plane's normal which has the cosines

$$\epsilon_1 = -\frac{1}{V}\frac{V_1V_3}{\sqrt{V_1^2+V_2^2}}, \quad \epsilon_2 = -\frac{1}{V}\frac{V_2V_3}{\sqrt{V_1^2+V_2^2}}, \quad \epsilon_3 = \frac{1}{V}\sqrt{V_1^2+V_2^2}. \tag{12}$$

With horizontal winds ($V_3 = 0$) this normal is pointing upward (in positive z-direction). In reference 1 therefore, the distance between horizontal planes had been kept within prescribed bounds in order to insure safe measurement. With inclined winds one would restrict the "layer thickness" in the analogous direction

$$\underline{\epsilon} = \underline{i}\epsilon_1 + \underline{j}\epsilon_2 + \underline{k}\epsilon_3.$$

It may then be defined as the ("cross") distance between two "restraining" planes* E through the ($k \leftrightarrow \ell$) and ($m \leftrightarrow n$) beam connections and is given by

$$\delta_{k\ell,mn} = \pm \underline{\epsilon} \cdot (\underline{r}^*_{k\ell} - \underline{r}^*_{mn}). \qquad (13)$$

For deriving expression (13) consider, quite generally, two parallel planes through arbitrary points P_1 and P_2:

$$\epsilon_1(x-x_1) + \epsilon_2(y-y_1) + \epsilon_3(z-z_1) = 0$$

$$\epsilon_1(x-x_2) + \epsilon_2(y-y_2) + \epsilon_3(z-z_2) = 0.$$

Their common normal through the origin,

$$\frac{x}{\epsilon_1} = \frac{y}{\epsilon_2} = \frac{z}{\epsilon_3},$$

intersects with the two planes at points with the coordinates

$$\xi_1 = \epsilon_1(\underline{\epsilon}\ \underline{r}_1), \quad \eta_1 = \epsilon_2(\underline{\epsilon}\ \underline{r}_1), \quad \zeta_1 = \epsilon_3(\underline{\epsilon}\ \underline{r}_1)$$

$$\xi_2 = \epsilon_1(\underline{\epsilon}\ \underline{r}_2), \quad \eta_2 = \epsilon_2(\underline{\epsilon}\ \underline{r}_2), \quad \zeta_2 = \epsilon_3(\underline{\epsilon}\ \underline{r}_2)$$

---

*These are parallel to each other, as identified by two pairs of parallel lines, each consisting of a beam connection and a normal to the vertical plane.

where

$$\underline{r}_i = \underline{i}x_i + \underline{j}y_i + \underline{k}z_i \qquad (i = 1,2)$$

are the position vectors of P_1 and P_2. The distance of the intersection points is

$$\sqrt{[(\underline{\epsilon}\ \underline{r}_1) - (\underline{\epsilon}\ \underline{r}_2)]^2(\epsilon_1^2 + \epsilon_2^2 + \epsilon_3^2)} = \sqrt{[\underline{\epsilon} \cdot (\underline{r}_1 - \underline{r}_2)]^2}$$

$$= \pm\ \underline{\epsilon} \cdot (\underline{r}_1 - \underline{r}_2).$$

IV. FOUR BASIC TRANSIT TRIADS

To develop the beam system's capability of measuring horizontal winds regardless of their direction is a foremost concern which will guide us in selecting basic triads from among the twenty operative.

Let us begin, quite modestly, with winds arriving from about the first quarter of the rose ($\varphi \approx 0° \ldots 45°$). Inspection of Figure 1 suggests to employ the beam connections

(ab), (dc), (db)

defining triad I. Indeed, with $V_3 = 0$, the first two are realized at height h when $\varphi = 45°$, the last one is so with $\varphi = 0°$. Note that all four beams are employed with these three transitions.* Relations (7) and (8) yield the equations

$$\begin{cases} -\dfrac{2\lambda s}{\tau^*_{ab}} = V_1(1+\lambda) + V_2(1-\lambda) + V_3\sigma(1+\lambda^2) \\ -\dfrac{2\lambda s}{\tau^*_{dc}} = V_1(1+\lambda) + V_2(1-\lambda) - V_3\sigma(1+\lambda^2) \qquad (\tau^*_{dc} = -\tau^*_{cd}) \\ -\dfrac{2\lambda s}{\tau^*_{db}} = V_1 - \lambda V_2 \quad (\tau^*_{db} = -\tau^*_{bd}) \end{cases} \qquad (14)$$

*The single transit triad of reference 1 uses three beams only, although in a highly asymmetric arrangement, to track horizontal winds arriving from a 90° azimuthal sector.

which can be resolved for the wind components:

$$\begin{cases} V_1 = -\dfrac{\lambda s}{1+\lambda^2}\left[\dfrac{\lambda}{\tau_1} + \dfrac{2(1-\lambda)}{\tau_2} + \dfrac{\lambda}{\tau_3}\right] \\ V_2 = -\dfrac{\lambda s}{1+\lambda^2}\left[\dfrac{1}{\tau_1} - \dfrac{2(1+\lambda)}{\tau_2} + \dfrac{1}{\tau_3}\right] \\ V_3 = -\dfrac{\lambda s}{1+\lambda^2}\,\dfrac{1}{\sigma}\left(\dfrac{1}{\tau_1} - \dfrac{1}{\tau_3}\right). \end{cases} \tag{15}$$

To prepare the way for concise formulations later on an abbreviated notation has been introduced here:

$$\tau^*_{ab} \equiv \tau_1, \quad \tau^*_{db} \equiv \tau_2, \quad \tau^*_{dc} \equiv \tau_3. \tag{15a}$$

Since the τ_i, and therefore the V_i, will be subject to certain admissibility conditions, the path length vectors $\underline{R}^*_{ab}$, $\underline{R}^*_{dc}$, and $\underline{R}^*_{db}$ constitute a vector set whose elements are bounded both in magnitude and direction. Taken together they fill a finite space region which may be termed the observation volume of winds accessible through triad I transits. Similar remarks hold for all triads. The overall observation volume thus is a composite body.

For dealing with the second half of the first quarter ($\varphi \approx 45° \ldots 90°$) a triad II composed of the transits

(ab), (dc), (ac)

will be suitable. At height h a horizontal wind with $\varphi = 45°$ again links a to b, d to c, while it connects a and c when $\varphi = 90°$ (Figure 1).

The formulas (8) and (9) here give

$$\begin{cases} -\dfrac{2\lambda s}{\tau^*_{ab}} = (1+\lambda)V_1 + (1-\lambda)V_2 + (1+\lambda^2)V_3\sigma \\ -\dfrac{2\lambda s}{\tau^*_{dc}} = (1+\lambda)V_1 + (1-\lambda)V_2 - (1+\lambda^2)V_3\sigma \\ -\dfrac{2\lambda s}{\tau^*_{ac}} = (\lambda V_1 + V_2), \end{cases} \tag{16}$$

which system resolves into

$$\left\{\begin{aligned} V_1 &= -\frac{\lambda s}{1+\lambda^2}\left[\frac{1}{\tau_1} - \frac{2(1-\lambda)}{\tau_2} + \frac{1}{\tau_3}\right] \\ V_2 &= -\frac{\lambda s}{1+\lambda^2}\left[-\frac{\lambda}{\tau_1} + \frac{2(1+\lambda)}{\tau_2} - \frac{\lambda}{\tau_3}\right] \\ V_3 &= -\frac{\lambda s}{1+\lambda^2}\,\frac{1}{\sigma}\left(\frac{1}{\tau_1} - \frac{1}{\tau_3}\right), \end{aligned}\right. \tag{17}$$

where

$$\tau_1 \equiv \tau^*_{ab}, \qquad \tau_2 \equiv \tau^*_{ac}, \qquad \tau_3 \equiv \tau^*_{dc}. \tag{17a}$$

Winds with $\varphi \approx 90° \ldots 135°$ will be handled by a transit triad III which can be obtained either as above or else from the triad I. The beams a, b, c, d used there will have to be rotated by 90° about the z-axis to go into b,c,d,a. Mathematically, this is equivalent to keeping the beams where they are and rotating the coordinate system by -90°. The original wind vector (5) then transforms into

$$\underline{V} = -\underline{j}V_1 + \underline{i}V_2 + \underline{k}V_3,$$

so that the former components V_1, V_2 have to be replaced by V_2, $-V_1$. From the solutions (15),

$$\left\{\begin{aligned} V_1 &= \frac{\lambda s}{1+\lambda^2}\left[\frac{1}{\tau_1} - \frac{2(1+\lambda)}{\tau_2} + \frac{1}{\tau_3}\right] \\ V_2 &= \frac{\lambda s}{1+\lambda^2}\left[-\frac{\lambda}{\tau_1} - \frac{2(1-\lambda)}{\tau_2} - \frac{\lambda}{\tau_3}\right] \\ V_3 &= \frac{\lambda s}{1+\lambda^2}\,\frac{1}{\sigma}\left(-\frac{1}{\tau_1} + \frac{1}{\tau_3}\right) \end{aligned}\right. \tag{18}$$

where

$$\tau_1 \equiv \tau^*_{bc}, \quad \tau_2 \equiv \tau^*_{ac}, \quad \tau_3 \equiv \tau^*_{ad} . \tag{18a}$$

The transits (bc), (ac), and (ad) are being used by the triad III.

In like manner, winds out of the sector $\varphi \approx 135° \ldots 180°$ are turned by 90° from those accessible by triad II. The triad IV appropriate for them will therefore consist of the transits

(bc), (ad), (bd).

Following the pattern (17), we find the velocity components as

$$\begin{cases} V_1 = \dfrac{\lambda s}{1+\lambda^2}\left(-\dfrac{\lambda}{\tau_1} + \dfrac{2(1+\lambda)}{\tau_2} - \dfrac{\lambda}{\tau_3}\right) \\ V_2 = \dfrac{\lambda s}{1+\lambda^2}\left(-\dfrac{1}{\tau_1} + \dfrac{2(1-\lambda)}{\tau_2} - \dfrac{1}{\tau_3}\right) \\ V_3 = \dfrac{\lambda s}{1+\lambda^2}\dfrac{1}{\sigma}\left(-\dfrac{1}{\tau_1} + \dfrac{1}{\tau_3}\right) \end{cases} \tag{19}$$

with

$$\tau_1 \equiv \tau^*_{bc}, \quad \tau_2 \equiv \tau^*_{bd}, \quad \tau_3 \equiv \tau^*_{ad}. \tag{19a}$$

The four triads are destined to monitor winds arriving from an aggregate angular sector $\varphi \approx 0° \ldots 180°$. The associate four groups of solutions are all of the same general form

$$V_1 = a_1\left(\frac{1}{\tau_1} + \frac{1}{\tau_3}\right) + \frac{a_2}{\tau_2} ,$$

$$V_2 = b_1\left(\frac{1}{\tau_1} + \frac{1}{\tau_3}\right) + \frac{b_2}{\tau_2}\ ,$$

$$V_3 = c_1\left(\frac{1}{\tau_1} - \frac{1}{\tau_3}\right)\ ,$$

a propitious circumstance that allows the use of the same four triads for $\varphi \approx 180° \ldots 360°$. This is seen as follows.

If a right-side wind vector is rotated by 180° about the z-axis, the V_3-component is preserved while the two others turn into their negative counterparts. The role of the beams a,b,c,d is taken over by the beams c,d,a,b, so that, especially, any τ_2 goes into $\tau_2' = -\tau_2$ (as $\tau^*_{nm} = -\tau^*_{mn}$). From the transformed solution system:

$$V_1' = -a_1\left(\frac{1}{\tau_1'} + \frac{1}{\tau_3'}\right) - \frac{a_2}{\tau_2'}$$

$$V_2' = -b_1\left(\frac{1}{\tau_1'} + \frac{1}{\tau_3'}\right) - \frac{b_2}{\tau_2'}$$

$$V_3' = c_1\left(\frac{1}{\tau_1'} - \frac{1}{\tau_3'}\right),$$

one concludes that among the remaining τ's the relation must hold

$$\text{(a)}\quad \frac{1}{\tau_1} - \frac{1}{\tau_3} = \frac{1}{\tau_1'} - \frac{1}{\tau_3'}\ ,$$

because $V_3' = V_3$. Since furthermore $\tan\varphi = \tan(\varphi + 180°)$ we have

$$\frac{V_2'}{V_1'} = \frac{V_2}{V_1}$$

which equality, together with $\tau_2' = -\tau_2$, leads to the link

$$\text{(b)}\quad \frac{1}{\tau_1'} + \frac{1}{\tau_3'} + \frac{1}{\tau_1} + \frac{1}{\tau_3} = 0.$$

From relations (a) and (b)

$$\tau_1' = -\tau_3, \ \tau_3' = -\tau_1.$$

Thus, any left-side wind covered by the primed system can be written as

$$V_1' = a_1\left(\frac{1}{\tau_3} + \frac{1}{\tau_1}\right) + \frac{a_2}{\tau_2}$$

$$V_2' = b_1\left(\frac{1}{\tau_3} + \frac{1}{\tau_1}\right) + \frac{a_2}{\tau_2}$$

$$V_3' = c_1\left(-\frac{1}{\tau_3} + \frac{1}{\tau_1}\right);$$

that is, it is also covered by the original system. If a certain set of τ_i defines a right-side wind, a left-side wind (the former turned by 180° about the z-axis) will be described by the set $-\tau_i$. It is again seen that, in correlating, one must delay both ways. Since four beams are employed, cross correlation of all six record combinations is called for. The travel times extricated are conveniently arranged in four sequences τ_1, τ_2, τ_3:

I (ab), (db), (dc)

II (ab), (ac), (dc)

III (bc), (ac), (ad)

IV (bc), (bd), (ad).

Note that the middle time-term of IV is oppositely equal to that of I. It is quite possible that some spaces are filled by several entries of which one alone (and at most) ought to be in the admissibility region. A moderately inclined wind will be discovered by the presence of an admissible travel time triad and can be computed from the pertaining solution group for its components.

Further discussion of travel times can concentrate on triads I and II that, taken together, are supposed to handle winds streaming toward the first quadrant. The results are also binding for the "rotated" triads III and IV (2nd quadrant)*, and, by simply inverting the transit time signs, for the entire left half of the rose as well.

The last line of the system (14)(triad I) requires that

$$V_1 - \lambda V_2 \neq 0,$$

because otherwise the travel time $\tau^*_{db} (\equiv \tau_2)$, and therefore the associated path length, would grow beyond all limits, clearly marking a physically prohibited situation. In particular, V_1 and V_2 are not allowed to be both zero, so that the measurement of vertical winds is not feasible.** Since we had provisionally assumed that triad I transits are used when

$$V_1 < V_2 \leqq 0,$$

the travel time τ_2 is positive. Continuing, we must distinguish between two cases. If first $V_3 \geqq 0$, $\tau^*_{dc} \equiv \tau_3$ is also positive; $\tau^*_{ab} \equiv \tau_1$ is so, provided that

$$V_3 \sigma(1+\lambda^2) < -V_1(1+\lambda) - V_2(1-\lambda). \qquad (20a)$$

The opposite requirement*** precludes the measurement of horizontal winds, in which the main interest of the present section resides. Secondly, with $V_3 \leqq 0$, τ_1 is positive by itself, while τ_3 will be found as positive if

$$-V_3 \sigma(1+\lambda^2) < -V_1(1+\lambda) - V_2(1-\lambda), \qquad (20b)$$

a condition satisfiable by horizontal winds.

---

* The relative positions of wind vectors and beam systems are the same as with I and II transits.

** It requires different triads, or perhaps an altogether different approach (as some preliminary investigations seem to suggest). To deal with strongly inclined winds must be relegated to later work.

*** It will be made in a later section.

Turning to the triad II which is supposed to govern winds with

$$V_2 < V_1 \leqq 0,$$

we see from the last line of the system (16) that $\tau^*_{ac} \equiv \tau_2$ is positive. The first two lines are identical with those of the system (14) so that the restraining conditions (20a) and (20b) again apply. All travel times are positive.

For right-side winds, they are also positive with triads III and IV which apply to the second quadrant in substituting V_2, $-V_1$ for V_1, V_2. The above inequalities are to be written accordingly.

Conversely, all travel times are negative with left-sided winds of a class that includes detectable horizontal winds. It is permissible to disregard such times as long as conditions (20) are upheld (which guarantee equal signs).

The conditions restrain the magnitude of $|V_3|$ and thereby limit the χ-ranges accessible to measurement. The mathematical formulation simplifies consequent on the fact that, by expression (10) and the solution systems, tan χ depends on the (positive) ratios

$$Q_1 = \frac{\tau_2}{\tau_1}, \qquad Q_3 = \frac{\tau_2}{\tau_3} \tag{21}$$

rather than on the τ_i themselves. With the abbreviations

$$D = Q_3 - Q_1, \qquad T = Q_1 + Q_3 - 2 \tag{22}$$

we first rewrite the four groups of solutions* as

*The particular choice (21) of time ratios has been suggested by the form of the expressions (15), (17), (18), and (19).

$$\begin{cases} V_1 = -\dfrac{\lambda s}{1+\lambda^2}\dfrac{1}{\tau_2}(2+\lambda T) \\ V_2 = -\dfrac{\lambda s}{1+\lambda^2}\dfrac{1}{\tau_2}(T-2\lambda) \\ V_3 = \dfrac{\lambda s}{1+\lambda^2}\dfrac{1}{\tau_2}\dfrac{D}{\sigma} \end{cases} \tag{23I}$$

$$\begin{cases} V_1 = -\dfrac{\lambda s}{1+\lambda^2}\dfrac{1}{\tau_2}(T+2\lambda) \\ V_2 = -\dfrac{\lambda s}{1+\lambda^2}\dfrac{1}{\tau_2}(2-\lambda T) \\ V_3 = \dfrac{\lambda s}{1+\lambda^2}\dfrac{1}{\tau_2}\dfrac{D}{\sigma} \end{cases} \tag{23II}$$

$$\begin{cases} V_1 = \dfrac{\lambda s}{1+\lambda^2}\dfrac{1}{\tau_2}(T-2\lambda) \\ V_2 = -\dfrac{\lambda s}{1+\lambda^2}\dfrac{1}{\tau_2}(2+\lambda T) \\ V_3 = \dfrac{\lambda s}{1+\lambda^2}\dfrac{1}{\tau_2}\dfrac{D}{\sigma} \end{cases} \tag{23III}$$

$$\begin{cases} V_1 = \dfrac{\lambda s}{1+\lambda^2}\dfrac{1}{\tau_2}(2-\lambda T) \\ V_2 = -\dfrac{\lambda s}{1+\lambda^2}\dfrac{1}{\tau_2}(T+2\lambda) \\ V_3 = \dfrac{\lambda s}{1+\lambda^2}\dfrac{1}{\tau_2}\dfrac{D}{\sigma} \quad . \end{cases} \tag{23IV}$$

With all four groups,

$$\sqrt{V_1^2 + V_2^2} = \frac{\lambda s}{\sqrt{1+\lambda^2}}\frac{1}{\tau_2}\sqrt{T^2+4} \; . \tag{24}$$

Since V_3 is also given by the same expression everywhere, a common formula

$$\tan \chi = \pm \frac{1}{\sigma \sqrt{1+\lambda^2}} \frac{D}{\sqrt{T^2+4}} \equiv \pm \frac{D \tan \psi}{\sqrt{T^2+4}} , \tag{25}$$

describes the χ-variation in the realms of the four basic triads.* The differences lie in the correlation of the number indices with the double-letter indices as spelled out by the identities (15a), (17a), (18a), and (19a).

Since through solutions (23) the restrictions (20) assume the form

$$D < T + 2 \qquad \text{if } V_3 \geqq 0$$

$$D > -T - 2 \qquad \text{if } V_3 \leqq 0,$$

upper bounds on the wind elevation appear in writing

$$|\tan \chi| < \frac{T+2}{\sqrt{T^2 + 4}} \tan \psi.$$

Once a value of ψ has been agreed upon, they are determined by the azimuthal angle alone; for so is the quantity T, as can be seen by the solutions (23).

A further significant conclusion can be drawn from these solutions. On putting them into the expressions (7) and (13), the time τ_2 cancels, so that the path length and cross distance restrictions imposed on the τ_i affect the values of T and D alone, that is, those of Q_1 and Q_3. Hence, the admissibility range of the τ_i can now be determined, more precisely, as a range of their ratios, Q_1 and Q_3, representing a certain area in the Q_1,Q_3-plane such that any point within it is defined by travel times compatible with the physical requirements for trustworthy

---

*The beam elevation angle ψ enters from the second of the relations (3). The sign depends on whether D/τ_2 is positive ($V_3 > 0$) or negative.

measurement. The next section is preparatory to delineating such an area, a task alleviated by the following observation.

From the four groups (23), it is seen that

$$\text{with } V_3 \geqq 0: \quad Q_3 \geqq Q_1 \ (> 0),$$

$$\text{with } V_3 \leqq 0: \quad Q_1 \geqq Q_3 \ (> 0).$$

Similar inequalities apply with left-sided winds. In any event, upward and downward motion merely differs in that Q_1 takes the role of Q_3 and vice versa. Since this exchange does not alter the value of T, any valid point Q_1, Q_3 on a line T = const. ($V_3 \geqq 0$) corresponds to a valid point, $Q_1' = Q_3$, $Q_3' = Q_1$, on the same line, at which $V_3 \leqq 0$. It suffices to develop the area in question for $V_3 \geqq 0$. That for $V_3 \leqq 0$ is simply its mirror image with respect to the axis $Q_1 = Q_3$ ($V_3 = 0$) which is orthogonal to the lines $T \equiv Q_1 + Q_3 - 2 = \text{const}$.

V. UNIFIED TREATMENT OF PATH LENGTHS AND CROSS DISTANCES (BASIC TRIADS)

All four solution groups yield formally the same expression for the wind speed:

$$V = \sqrt{V_1^2 + V_2^2}\sqrt{1 + \tan^2\chi} = \frac{\lambda s}{\sqrt{1+\lambda^2}} \frac{1}{\tau_2} \sqrt{T^2 + 4 + D^2\tan^2\psi}, \tag{26}$$

as follows directly from relations (24) and (25). With the latter the positive sign applies in the case taken up here where $V_3 \geqq 0$ ($D \geqq 0$).

The path lengths pertaining to the transits in any of the four triads may be written as

$$R_i^* = \tau_i V \qquad (i = 1,2,3),$$

or, more explicitly, as

$$R_1^* = \frac{\lambda s}{\sqrt{1+\lambda^2}} \frac{1}{Q_1} \sqrt{T^2 + 4 + D^2 \tan^2\psi}$$

$$R_2^* = \frac{\lambda s}{\sqrt{1+\lambda^2}} \sqrt{T^2 + 4 + D^2 \tan^2\psi} \qquad (27)$$

$$R_3^* = \frac{\lambda s}{\sqrt{1+\lambda^2}} \frac{1}{Q_3} \sqrt{T^2 + 4 + D^2 \tan^2\psi}$$

where the earlier correspondences between number- and letter-indices can be used to return to a particular triad. Since by relations (3)

$$\frac{\lambda s}{\sqrt{1+\lambda^2}} = \frac{\lambda h}{1+\lambda^2} \cot \psi, \qquad (28)$$

the paths are seen to wax longer with less inclined beams, provided the height, h, of the square aloft is kept fixed. This behavior appears as evident geometrically. With $V_3 > 0$ the path R_3^* is always shorter than R_1^*; R_2^* can be shorter or longer than both, or have an intermediate length.

The solution groups (23III) and (23IV) were obtained from the preceding two groups by rotations which cannot alter the measure of a length. It is therefore sufficient to deal with the first two transit triads when deriving the needed expressions for the cross distances. We wish to learn besides which of them is largest in given circumstances, and for this reason, is to be kept in bounds.

From the general result (13) the distances*

$$\delta_{ab,db} = \underline{\epsilon} \cdot (\underline{r}_{ab}^* - \underline{r}_{db}^*)$$

$$\delta_{db,dc} = \underline{\epsilon} \cdot (\underline{r}_{db}^* - r_{dc}^*)$$

$$\delta_{dc,ab} = \underline{\epsilon} \cdot (\underline{r}_{dc}^* - \underline{r}_{ab}^*)$$

---

*The double signs have been removed as irrelevant in the present context.

have to be compared in the triad I of $a \leftrightarrow b$, $d \leftrightarrow b$, $d \leftrightarrow c$ transits. The sum of the right sides being zero, one distance balances the two others. Marked by a sign opposite to theirs, it is the one to be suitably restricted.

With the aid of relations (6), (12), (10), and (23I), the δ-expressions can be rearranged to give

$$\begin{cases} \delta_{ab,db} = -\dfrac{2\lambda h \cos\chi}{1+\lambda^2}\,\dfrac{xT+1-x^2)(2+xT)}{(1+x)(T^2+4)} \equiv -\delta_{12} \\[2ex] \delta_{db,dc} = \dfrac{2\lambda h \cos\chi}{1+\lambda^2}\,\dfrac{(xT+1-x^2)(T^2-xT+2)}{(T+1-x)(T^2+4)} \equiv \delta_{23} \\[2ex] \delta_{dc,ab} = -\dfrac{2\lambda h \cos\chi}{1+\lambda^2}\,\dfrac{(xT+1-x^2)(T-2)(T-2x)}{(1+x)(T+1-x)(T^2+4)} \equiv -\delta_{31} \end{cases} \tag{29}$$

where

$$x = Q_1 - 1. \tag{29a}$$

To judge the relative wind layer thicknesses (cross distances), it suffices to examine the aggregates

$$A = -\frac{2+xT}{1+x} \equiv -\frac{(2-T)+TQ_1}{1+x}$$

$$B = \frac{T^2-xT+2}{T+1-x}$$

$$C = -\frac{(T-2)(T-2x)}{(1+x)(T+1-x)}\ .$$

From $Q_3 \geqq Q_1$ ($V_3 \geqq 0$) one infers that $T \geqq 2x$ and therefore

$$T+1-x \geqq 1+x = Q_1 > 0.$$

The three denominators thus are positive.

The numerator of B may be put into two forms:

$$T^2-xT+2 = \begin{cases} T(Q_3-1) + 2 > 0 & \text{when } T \geqq 0 \\ (T - \frac{1}{2} x)^2 + 2 - \frac{1}{4} x^2 > 0 & \text{when } T \leqq 0. \end{cases}$$

The first statement is true, since with $T \geqq 0$ and $Q_3 \geqq Q_1$, the ratio Q_3 is at least equal to unity. The second is based on the fact that if T is negative the difference $x \leqq T/2$ is so, too, but remains larger than -1 (as $Q_1 > 0$). One concludes that $B > 0$.

The signs of B, A, and C prove

Rule I: If $T \leqq 2$, restrict the thickness $|\delta_{12}|$.

For $A < 0$, $C \geqq 0$ then. With $T > 2$, however, C is negative. As a consequence,

Rule IIA: If $T > 2$ and $2+xT > 0$, restrict thickness $|\delta_{23}|$.

Rule IIB: If $T > 2$ and $2+xT < 0$, restrict thickness $|\delta_{31}|$.

With the solutions (23I)

$$\tan \varphi_I = \frac{T-2\lambda}{\lambda T+2}, \tag{30}$$

so that the main dividing line $T = 2$, or $Q_1 + Q_3 = 4$, corresponds to

$$\tan \varphi_I^* = \frac{1-\lambda}{1+\lambda},$$

i.e., to an azimuth smaller than 45° (depending on the value chosen for $\lambda < 1$).

Furthermore, since $x = \frac{T-D}{2}$, the condition $2+xT > 0$ may be written as

$$D < \frac{T^2-4}{T}$$

and thus refers to the wind elevation. It must be sufficiently small:

$$\tan \chi < \frac{T^2-4}{T\sqrt{T^2+4}} \tan \psi$$

if rule IIA rather than rule IIB is to apply.

The beam connections constituting the second triad define the cross distances:

$$\delta_{ab,ac} = \underline{\epsilon} \cdot (\underline{r}^*_{ab} - \underline{r}^*_{ac})$$

$$\delta_{ac,dc} = \underline{\epsilon} \cdot (\underline{r}^*_{ac} - \underline{r}^*_{dc})$$

$$\delta_{dc,ab} = \underline{\epsilon} \cdot (\underline{r}^*_{dc} - r^*_{ab}),$$

whose sum is zero again.

For rearrangement we may use the same formulas except that (23II) enters for (23I). In the final outcome

$$\delta_{ab,ac} = \delta_{12}$$

$$\delta_{ac,dc} = -\delta_{23}$$

$$\delta_{dc,ab} = \delta_{31}.$$

In other words, these distances, aside from sign inversion, are given by expressions formally identical with those of the first triad. Owing to this lucky circumstance, the rules derived above are also applicable with triad II transits, consequently with all transit combinations introduced as yet. Since the path length expressions are also formally alike for the four triads, the admissibility area, insofar as it depends on physical restrictions, can be established once for all in taking the first triad as representative. This rather remarkable result, which saves a great deal of intricate work, is doubtless due to the symmetry of the geometrical arrangement.

The individual triad, as we know, reappears as soon as the common symbol T is interpreted in terms of azimuths. With triad II, e.g.,

$$\tan \varphi_{II} = \frac{2-\lambda T}{T+2\lambda}, \tag{31}$$

an expression different from that holding with triad I (although the critical value T = 2 again corresponds to $\tan \varphi^{*}_{II} = \frac{1-\lambda}{1+\lambda}$).

The puzzling sign discrepancy in the two results found for $\delta_{dc,ab}$ is founded in the different φ-ranges for which triads I and II are responsible.* Where they overlap, the value of the distance comes out as the same for the same wind.

For illustration, take $\varphi_I = \varphi_{II} = 45°$ corresponding to

$$T_I = 2\,\frac{1+\lambda}{1-\lambda}, \qquad T_{II} = 2\,\frac{1-\lambda}{1+\lambda}.$$

Writing T-2x for D in relation (25), we may obtain a common value of χ by putting $\tan \chi_I = \tan \chi_{II}$ or

$$\lambda - (1-\lambda)\, x_I = -\lambda - (1+\lambda)\, x_{II}.$$

From among the many elevation angles conceivable, let us select the one associated with

$$x_I = \frac{\lambda}{1-\lambda}, \qquad x_{II} = -\frac{\lambda}{1+\lambda} \qquad \left(\tan \chi = \frac{1}{\sqrt{2}}\,\frac{1}{\sigma(1+\lambda^2)}\right).$$

The last expression in the set (29) then gives

*The same original expression was worked on with two different sets of expressions for the velocity components (and thus might have transformed quite differently, not ending up with just a sign exchange).

$$\delta_{31} = \frac{2\lambda h \cos\chi}{1+\lambda^2} \frac{\lambda(1+2\lambda^2)}{3(1+\lambda^2)} \quad \text{(triad I)},$$

while with triad II values,

$$\delta_{31} = -\frac{2\lambda h \cos\chi}{1+\lambda^2} \frac{\lambda(1+2\lambda^2)}{3(1+\lambda^2)} ,$$

so that indeed the distance $\delta_{dc,ab}$ has the same (negative) magnitude.

VI. (Q_1,Q_3)-PAIRS ADMISSIBLE WITH BASIC TRIAD TRANSITS

As was pointed out in the introduction, the straight eddy traces in between beams should neither be too short nor too long, nor should they define restraining planes too far distant from each other. These requirements are physical in nature and must be held more important than the need for error transmission limitation. Moreover, they supply all the information necessary four bounding off the admissibility area. Of course, if the error estimates (later to be made) run too high, one would have either to cut back the area or to check into and perhaps modify the numerical assumptions which, avoided so far, must now be made.

The boundary sought depends both on T and D, that is, on wind azimuth and elevation. The physical question therefore is: Which "elevation" D can be tolerated at any given "azimuth" T? By definitions (22),

$$\begin{aligned} Q_1 &= \frac{T+2-D}{2} \\ Q_3 &= \frac{T+2+D}{2} , \end{aligned} \qquad (32)$$

suggesting an alternative formulation of the problem: Given the line

$$T = Q_1 + Q_3 - 2 = \text{const.},$$

which points Q_1,Q_3 on it are admissible?

With Q_3 and Q_1 plotted on the horizontal and vertical axes, respectively, the admissibility area for $V_3 \geqq 0$ is some portion of the upper right quadrant in which $Q_1 \leqq Q_3$. According to relations (32) increasing elevation at φ = const. causes the point Q_1,Q_3 to slide down on the corresponding line T = const., whose inclination angle is 135 degrees. However, there is clearly an end to this motion. If D grows as large as T+2, Q_1 attains the value zero which is not acceptable.

Observing that the path length R_1^* increases beyond all bounds as Q_1 approaches zero, we start with limiting it by a suitable largest length, $\hat{R}$. Since by the first expressions (27) and (32) the path R_1^* increases with D, the solution $D = \hat{D}(T)$ which satisfies the equation $R_1^* = \hat{R}$ represents the largest value of D admissible at a given T. The corresponding smallest value, $Q_1 = \check{Q}_1(T)$, can be computed from relations (32), as well as the associated value, $Q_3 = \hat{Q}_3(T)$, largest on the given line T = const. An arc of the lower boundary curve* will be traced out by these line terminals.

Actual calculation must await parameter identification; however, a significant point related to the argument can be made without it.

With $V_3 \geqq 0$, the quantity Q_3, by the second relation (32), is larger than (or equal to) unity at least with $T \geqq 0$,** since $D = Q_3 - Q_1 \geqq 0$. The path R_3^* here may always be taken as the shortest of the three. Along any line T = const. it can be shown to decrease as D increases, certainly as long as $\tan \psi \leqq 2^{-0.5}$. By an independent reasoning it appears as plausible that this condition will have to be imposed on the beam elevation anyway; in fact, the value eventually chosen for ψ does satisfy it. Taking this for granted, we conclude that the short path R_3^* is shortest along the lower area boundary. Its variation along the arc $R_1^* = \hat{R}$ exhibits a surprising property: At T = 2 the path R_3^* assumes a minimum length regardless of the values the still undetermined parameters may have; they drop out of the equation for the extremum. It can be shown that the lower terminal of the line T = 2 is among those determined by the condition $R_1^* = \hat{R}$ rather than by some other of the physical restrictions. The result thence is meaningful.

At this station it becomes necessary to introduce a first numerical value. Let us assume we wish to measure a 20 m/sec wind ($\approx$ 40 knots)

---

*It is composed of several arcs, as will be seen presently.

**Earlier the φ-range subjected to triad I transits had been loosely defined as $\varphi_I \approx 0° \ldots 45°$. In accepting T = 0, we extend it down to $\varphi_I = -\arctan \lambda$, since expression (30) decreases with T.

even if it should happen to blow parallel to the shortest of all possible eddy tracks. Because the minimum transit time we are prepared to admit is one second, the latter must be assigned the length 20 m. Thus, at the terminal T = 2, D = $\hat{D}(2)$, two conditions have to be satisfied:

$$R_1^* = \hat{R}, \qquad R_3^* = 20,$$

from which the unknown quantity $\hat{D}(2)$ can be eliminated. A relationship of three parameters ensues:

$$\frac{\lambda s}{\sqrt{1+\lambda^2}} \sqrt{2(\hat{R}+20)^2 + 4(\hat{R}-20)^2 \tan^2\psi} = 40\hat{R}. \tag{33}$$

A definite value will eventually be selected for the largest path length $\hat{R}$ we are going to tolerate. Nevertheless, the quantities

$$\frac{\lambda s}{\sqrt{1+\lambda^2}} \quad \text{and} \quad \psi ,$$

instrumental in shaping detector layout and beam configuration, cannot be found as yet. Needed further information issues from the basic demand to insure the measurement of horizontal winds at least up to the azimuth 45°. Accordingly, by expression (30), one must see to it that the T-range at least extends to

$$T = 2\,\frac{1+\lambda}{1-\lambda} . \tag{34}$$

Even if the λ-interval is narrowed down to

$$0 < \lambda \leqq \frac{1}{4} , \tag{35}$$

the minimum requirement is $T = 10/3 \equiv T.^*$

With horizontal winds ($Q_1 = Q_3$), we have $T = 2x$ and therefore $\delta_{31} = 0$,

$$\delta_{12} = \delta_{23} = \frac{\lambda h}{1+\lambda^2} \frac{T^2+4}{2(T+2)} \ . \tag{36}$$

The T-function has a minimum at $T = 2(\sqrt{2}-1) < T^*$. If we accept, as a second numerical limit, that cross distances should not exceed 16 m*, the value of T^* implies that the parametric factor should be chosen below 11.3. Deciding also on a value for $\hat{R}$,** we put

$$\frac{\lambda h}{1+\lambda^2} = 11 \text{ m}, \qquad \hat{R} = 154 \text{ m}. \tag{37}$$

Relation (28) transforms the root factor in equation (33), which then has the (almost exact) solution

$$\tan \psi = \frac{1}{2} \ , \tag{38}$$

the beam inclination becoming ≈ 26.5 degrees.

To the figures (37) and (38), we add, for convenience, a related figure following from the equality (28):

$$\frac{\lambda s}{\sqrt{1+\lambda^2}} = 22 \text{ m}. \tag{39}$$

These results, to recapitulate, reflect numerical assumptions on the shortest travel time (made for error containment), on the maximal wind speed expected, on the largest cross distance and path length allowable, and on the variation permitted for the relative size, characterized by λ, of the squares on ground and aloft. The need for overlapping φ-ranges (to measure horizontal winds arriving from any

---

* In reference 1, as much as 18 m was considered tolerable.

**Clear-cut brackets for it are hard to come by. The figure chosen seems reasonable and leads to the smooth result (38).

direction whatsoever) has been taken care of, but no figure has been placed on reference height which, by relations (37) and (39), would finally identify detector positions. The admissibility area can be developed without it.

Of it we so far merely know that some part of its lower boundary follows from the condition $R_1^* = 154$ m. If $\tilde{Q}_1(T)$ reaches unity, the path R_2^* becomes the longest, and the condition is relieved by $R_2^* = 154$ m. With the parameter figures as established, this happens at $T = 6$. The altered restraint causes a sharp break (discontinuous tangent) to appear at the point $\tilde{Q}_1 = 1$, $\hat{Q}_3 = 7$. In proceeding to even larger values of T (and $\tilde{Q}_1$), one has to watch the cross distance δ_{23} which, by Rule IIA, is the largest of the three here. At $T = 6.32$ already, this thickness arrives at its limit (16 m), stopping further increase of T and continuation of the lower boundary. The end point has the coordinates $\hat{Q}_3 = 6.40$, $\tilde{Q}_1 = 1.92$.

The opposite end point, too, is not controlled by the condition $R_1^* = 154$ m, although it is still operative at $T = 2$ and values below. The distance requirement $\delta_{12} = 16$ m, which must be heeded according to Rule I, takes over at $T = 0.0516$ ($\hat{Q}_3 = 1.747$, $\tilde{Q}_1 = 0.304$), where the lower boundary suffers another break. At $T = -0.529$* it reaches the line $D = 0$ ($\hat{Q}_3 = \tilde{Q}_1 = 0.736$) and its natural end. Any value below $T = -0.529$ would violate the δ_{12}-restriction (which also applies along $D = 0$, where δ_{12} takes the form (36)).

The upper part of the boundary, defined by the upper terminals of the lines T = const.** starts at the lower part's end point $\hat{Q}_3 = 6.40$ ($=\tilde{Q}_3$), $\tilde{Q}_1 = 1.92$ ($=\hat{Q}_1$).*** The δ_{23}-restriction ruling there remains responsible all the way down from $T = 6.32$ to $T = 3.348$, when δ_{23} becomes identical with δ_{12}, and the upper boundary arrives at the line $D = 0$ ending there ($\tilde{Q}_3 = \hat{Q}_1 = 2.72$). This straight line, incidentally, is not part of the boundary; Figure 3 depicts one half of the area only which continues across $D = 0$ into the realm of downward winds, as was pointed out earlier. The total area is bounded by curved arcs everywhere, which appear in symmetric pairs.

---

* Rule I keeps in force when T drops below the zero point.

** Here $Q_3 = \tilde{Q}_3$ is smallest and $Q_1 = \hat{Q}_1$ is largest.

*** There is only one point admissible on T = 6.3, which therefore is both lowest and topmost.

One gathers from the foregoing that horizontal winds can be detected in the interval $-0.529 \leqq T \leqq 3.348$. The associated φ-values are found from expressions (30), (31), and two similar ones, depending on which of the four triads is operative.

Table I gives a number of lower boundary points together with the largest elevation angle that can be measured at the pertaining azimuths, and adds some other interesting information. Note especially the rapid growth of δ_{23} when $T > 6$.

TABLE I. Lower Boundary of Admissibility Area (Basic Triads)

T	$\hat{Q}_3$	$\tilde{Q}_1$	$\hat{\chi}°$	R_3^*(m)	δ_{23}(m)
-0.529	0.736	0.736	0	-	-
-0.5	0.77	0.73	0.6	-	-
-0.4	0.89	0.71	2.5	-	-
-0.2	1.14	0.66	6.8	-	-
0	1.5	0.5	14	-	-
0.05	1.74	0.31	19.6	-	-
0.2	1.892	0.308	21.5	24.7	-
0.5	2.177	0.322	24.2	22.8	-
1	2.641	0.359	27.0	20.9	-
1.5	3.095	0.405	28.3	20.2	-
2	3.54	0.46	28.9	20.0	-
2.5	3.98	0.52	28.5	20.1	-
3	4.42	0.58	28.0	20.2	-
3.5	4.851	0.649	27.5	20.6	-
4	5.283	0.717	27.0	21.0	-
5	6.143	0.857	26.1	21.5	-
6	7	1	25.4	22.0	-
6.1	6.84	1.26	23.9	22.5	6.8
6.2	6.66	1.54	21.5	23.1	10.9
6.32	6.40	1.92	18.7	24.0	16.0

It may be thought unsatisfactory that at the lowest T's winds with but small elevation angles can be handled. Here, however, the triad I transits can be supplemented by those of the triad IV* which, as we know, are useable in the second half (roughly) of the fourth azimuthal quadrant. The negative values of φ_I associated with $T_I \leqq 0$ are equivalent to $\varphi_{IV} = 360 + \varphi_I$. By solutions (23IV) and (23I)

$$\tan \varphi_{IV} = \frac{T_{IV} + 2\lambda}{\lambda T_{IV} - 2} = \tan \varphi_I = \frac{T_I - 2\lambda}{\lambda T_I + 2}$$

so that

$$T_{IV} = -T_I.$$

Although with triad I the "azimuth" $T_I = -0.5$ goes with very small wind elevations only, triad IV, at the "same azimuth" $T_{IV} = 0.5$, enables us to observe slant angles up to 24 degrees. Clearly, the lowest upper limit is $\hat{\chi} = 14°$ (at $T_I = T_{IV} = 0$). That in fact the arrangement is capable of measuring considerably larger elevations will be explained in subsequent sections.

The upper arc of the boundary is marked out by terminals of lines $T > 3.438$, so that winds accessible at these azimuths to triad I transits can never be horizontal.** Table II lists a few of the upper arc points and the smallest elevation angle measurable at the equivalent azimuths. The longest path, R_2^*, reaches 154 m at T = 6.3; larger T's would increase it beyond that limit.

TABLE II. Upper Boundary of Admissibility Area (Basic Triads)

T	3.438	3.5	4	5	6	6.3
$\tilde{Q}_3$	2.72	3.10	3.86	5.02	6.07	6.40
$\hat{Q}_1$	2.72	2.40	2.14	1.98	1.93	1.92
$\check{\chi}°$	0.0	4.0	10.9	15.7	18.1	18.7
R_2^*(m)	87.5	89.1	100	123	147	154

---

* Table I and the later Table II are applicable with all four triads of the basic group. The same admissibility area holds for all of them.

** Horizontal winds are detected by triad II transits. One finds readily that T_I and $T_{II} = 4/T_I$ define the same azimuth.

In computing the boundary the pertinent, i.e., the most demanding restraint, has of course been sought out and used. In the interior the path length functions, being on T = const. monotonic between boundary points, cannot have values outside the realm 20 m ... 154 m. The cross distance functions may exhibit a maximum as one learns by the usual method. Numerical computations made along suitably spaced T-lines on which it occurs have shown that, notwithstanding, the δ-values there remain sufficiently small. From their slowly changing, continuous character it is safe to infer that in between they will not exceed the prescribed limit either. By Tables I and II the layer thickness $|\delta_{31}|$ can never be the largest and was not considered; with $T > 2$ the sum $2+xT$ cannot become negative as required by Rule IIB.

VII. ERROR ESTIMATES (BASIC TRIADS)

In investigating errors one will seek to set up expressions for the worst that can possibly be expected to occur within the admissibility area. It will soon be seen that it suffices to consider one half of it, e.g., where $D = Q_3 - Q_1 \geqq 0$ $(\tau_1 \geqq \tau_3)$.*

The worst experimental error was taken as

$$|\Delta\tau_i| = 0.1 \text{ sec.}$$

The analytic expressions for V, tan φ, tan χ contain the quantities τ_2, T, D; that is, they depend on the three τ_i, which for the sake of argument will (and can) be taken as positive (winds arriving from right-hand directions). In a first approximation

$$|\Delta\tau_i| \approx |d\tau_i|.$$

From the definitions (21) and (22) one deduces that

$$dT = \frac{(T+2)d\tau_2 - Q_1^2 d\tau_1 - Q_3^2 d\tau_3}{\tau_2}$$

$$dD = \frac{Dd\tau_2 + Q_1^2 d\tau_1 - Q_3^2 d\tau_3}{\tau_2}. \qquad (40)$$

*It is depicted on Figure 3.

These errors estimated for T and D increase when τ_2 decreases. The smallest value permitted, $\tau_2 = 1$, can be used if $Q_3 \leqq 1$, for then $\tau_3 \geqq 1$, $\tau_1 \geqq \tau_3 \geqq 1$. The pertaining points Q_1, Q_3 are assembled in a small region near the lower terminal of the line $D = 0$. Putting $\tau_2 = 1$ when $Q_3 > 1$ is prohibited as τ_3 would become smaller than unity. Rather, one should take $\tau_3 = 1$, so that $\tau_2 = Q_3 > 1$. Also, $\tau_1 \geqq 1$.

It is seen that the restriction on travel time indeed serves to reduce the transmitted errors. A stipulation of this kind is necessary for their appraisal in general terms. However, a measurement exhibiting travel times less than unity need not be discarded out of hand if one is willing to test its reliability by calculating the particular errors involved.* The small denominators might be compensated for by sufficiently small numerators.

From all four solution groups (23) the strength of the wind emerges as the same expression,

$$V = \frac{\lambda s}{\sqrt{1+\lambda^2}} \frac{\sqrt{T^2+4 + D^2 \tan^2\psi}}{\tau_2} ,$$

where

$$\tan^2\psi = \frac{1}{\sigma^2(1+\lambda^2)}$$

is a constant, while T, D, and τ_2 are variables. Through logarithmic differentiation and application of expressions (40), one finds that

$$\frac{dV}{V} = \frac{1}{\tau_2} \frac{2(T-2)d\tau_2 - Q_1^2(T-D \tan^2\psi)d\tau_1 - Q_3^2(T+D \tan^2\psi)d\tau_3}{T^2 + 4 + D^2 \tan^2\psi} .$$

On putting $|d\tau_i| = 0.1$ and $\tan^2\psi = 1/4$, an estimate for the largest possible strength errors may be set down as

---

*Before doing this one should of course ascertain that the Q_i-values found define an admissible point.

$$\left(\frac{\Delta V}{V}\right)_{\text{larg.}} \approx \frac{1}{10\tau_2} \frac{2|T-2| + Q_1^2 \left|T - \frac{D}{4}\right| + Q_3^2 \left|T + \frac{D}{4}\right|}{T^2 + 4 + \frac{D^2}{4}}. \tag{41}$$

With $D < 0$ the roles of Q_1 and Q_3 are interchanged without altering the expression. Systematic numerical calculations have shown that the percent error estimate (41) is largest on the axis $D = 0$ of horizontal winds where it can go up to 13 percent (near its lower terminal point). Elsewhere, and more commonly, largest errors lie around 11 percent. They are as low as 7 percent in some instances (where then the one or other travel time somewhat smaller than unity may be tolerated, provided that the φ- and χ-errors stay also low enough).

The "worst" errors as defined presuppose: (1) maximum observational τ_i-errors committed such that (2) their contributions add up, and (3) strong winds (small τ_i's). These three conditions will not often be realized simultaneously. It does not seem worthwhile to cut off, for example, the tip farthest at left of the admissibility area merely to avoid the relatively large strength error that might occur there in a combination of unfavorable circumstances.* In addition, the wind pertaining to the tip can be measured both through triad I and triad IV transits; in the latter case the worst conceivable error was found as ~ 8.5 percent.

Although the expressions for $\tan \varphi = V_2/V_1$ are different in the four solution groups (23), the differential

$$d\varphi = \pm \frac{2}{T^2+4} \, dT$$

is essentially the same, so that one error evaluation only is needed. With the aid of the first relation (40), we may write the worst-error estimate as

$$(\Delta\varphi)_{\text{larg.}} \approx \frac{1}{5\tau_2} \frac{Q_1 + Q_3 + Q_1^2 + Q_3^2}{T^2+4}. \tag{42}$$

It clearly holds with $D > 0$ and $D < 0$ alike. Values for admissible points range from ~ 2 to ~ 12 degrees and should not cause concern.

---

*If all conditions are met with except that $\Delta\tau_1 = -\Delta\tau_3$, the error already reduces to 11.7 percent.

As to the elevation angle, relations (25) and (40) yield

$$d\chi = \frac{1}{\tau_2} \frac{D(2-T)d\tau_2 + Q_1^2[T(Q_3-1)+2]d\tau_1 - Q_3^2[T(Q_1-1)+2]d\tau_3}{\sqrt{T^2+4}\ (T^2 + 4 + \frac{D^2}{4})}$$

so that

$$(\Delta\chi)_{\text{larg.}} \approx \frac{1}{10\tau_2} \frac{|D(2-T)| + Q_1^2|T(Q_3-1)+2| + Q_3^2|T(Q_1-1)+2|}{\sqrt{T^2+4}\ (T^2 + 4 + \frac{D^2}{4})} \ . \qquad (43)$$

Evaluation of this formula (which is applicable with $D \gtrless 0$) yielded estimated error values often insignificant and at most ~ 4 degrees.

VIII. ADDITIONAL OBSERVATIONS THROUGH THE BASIC TRIADS

On inverting conditions (20) a number of nonhorizontal wind arrays should be found accessible to measurement. As was shown in general, the investigation can be restricted to triad I transits.

Condition (20a) applied with $V_3 \geqq 0$. Let us replace it by the opposite requirement:

$$(1+\lambda)V_{3\sigma} > -(1+\lambda)V_1 - (1-\lambda)V_2 > 0,$$

so that, from the two first lines of system (14),

$$\tau^*_{ab} \equiv \tau_1 < 0, \qquad \tau^*_{dc} \equiv \tau_3 > 0.$$

The third time, $\tau^*_{db} \equiv \tau_2$, can be either positive or negative; no condition for it exists. In either case Q_1 and Q_3 are of opposite signs.

Inverting the requirement (20b) associated with $V_3 \leqq 0$,

$$(1+\lambda^2)V_{3\sigma} < (1+\lambda)V_1 + (1-\lambda)V_2 < 0,$$

we find that

$$\tau^*_{dc} \equiv \tau_3 < 0, \qquad \tau^*_{ab} \equiv \tau_1 > 0.$$

Again, whether we take τ_2 positive or negative, Q_1 and Q_3 have different signs. The admissibility area will be determined with $Q_1 < 0$, $Q_3 > 0$; it has a symmetric counterpart mirrored at the axis $D = 0$, so that the former Q_1 assumes the role of Q_3 and vice versa.

Q_1 must not approach zero indefinitely. We will have to satisfy the condition

$$R^*_1 = 22 \frac{\sqrt{T^2 + 4 + \frac{(T-2x)^2}{4}}}{-(1+x)} \leqq 154.$$

Spot checks with $T = 0,1,2,3$ have shown that if $R^*_1 \leqq 154$, one of the thickness conditions is always violated. One may expect this to be true for all positive values of T.

In carving out the admissibility area for $T < 0$ one must consider the earlier expressions

$$A = \frac{2+T(Q_1-1)}{-Q_1}$$

$$B = \frac{2+T(Q_3-1)}{Q_3}$$

$$C = \frac{(T-2)(Q_3-Q_1)}{-Q_1Q_3}$$

whose denominators are all positive. Hence, $A > 0$, $C < 0$. Depending on whether the B-numerator

$$2+ T(Q_3-1)$$

is larger or smaller than zero one will have to restrict either $|\delta_{31}|$ or $|\delta_{12}|$. The area is depicted on Figure 4, where those parts of its boundary where a path length restriction is dominant are also indicated.

The worst transmission errors estimated to occur within the area go up to 12 percent in strength, to 7 percent in azimuth, and to 5.5 degrees in elevation angle. The error structure seems acceptable.

Since the useable T-range was determined as

$$-6 \leqq T \leqq -0.3,$$

the system (23I) tells that with $\tau_2 > 0$ the wind is directed toward the fourth quadrant blowing upward (downward) with $D > 0$ ($D < 0$). Opposite winds are present when $\tau_2 < 0$. The same conclusions can be drawn from the system (23II). Both the triads I and II thus measure an additional class of winds approaching the fourth and second quadrants. One finds that the azimuthal validity ranges overlap in large measure. However, V_2 can never become zero, nor can V_1, unless λ is relatively large. That is, the triads are, as a rule, not geared to the measurement of winds whose horizontal components are either parallel or antiparallel to one of the coordinate axes. Since the same is true of the triads III and IV that govern overlapping azimuthal reaches in the first and third quadrants, the upper bound of the measurable elevation angle remains at its rather low value ($\approx 14°$) for winds with $\varphi \approx 0°$ (90°) and $\varphi \approx 90°$ (270°).* To see its rise with other directions let us compare upward winds amenable to I, II, and III transits, provided that with the latter $\tau_1 < 0$, $\tau_2 > 0$, $\tau_3 > 0$. By the sets (23I), (23II), (23III) equal azimuths require that

$$T_I \, T_{III} = -4, \quad T_{III} = -T_{II}.$$

The values of χ defined by the intersection points of the line T_{III} = const. with the area boundary give the lower and upper bound of the χ-range available at the pertaining azimuth. Some of them are listed in the following table. For easy comparison the corresponding brackets with triad I and II transits are taken over from Tables I and II.

---

*A remedy for this is offered in the next section.

TABLE III. Measurable χ-Ranges (Basic Triads)

T_{III}	-0.8	-1	-4/3	-3/2
χ°_{III}	23.6 ... 33.2	22.2 ... 33.7	21.4 ... 34.0	21.1 ... 34.0
χ°_{I}	15.7 ... 26.1	10.9 ... 27.0	0 ... 28.0	0 ...~28.5
χ°_{II}	0 ...~ 26	0 ... 27.0	0 ...~ 28	0 ... 28.3

T_{III}	-2	-8/3	-3	-4	-5
χ°_{III}	20.9...33.8	21.1... 33.7	21.5...33.4	22.2...32.6	22.9...31.8
χ°_{I}	0 ...28.6	0 ... 28.3	0 ...~28°	0 ...27.0	0 ...~ 26
χ°_{II}	0 ...28.6	0 ...~28.5	0 ... 28°	10.9...27.0	15.7...26.1

It appears that at all azimuths permitted by added III-transits one can measure eddy tracks with elevation angles from 0° to well over 30°. In many instances a wind can be obtained in two or even three ways, for instance, if it blows at the azimuth $T_{III} = -4$ ($T_I = 1$, $T_{II} = 4$) with an elevation angle around 25 degrees. With $\chi > 28.6$ degrees but a single observation can be made.

IX. AUXILIARY TRIADS

Among the twenty triads of beam-connecting eddy paths, four use the same beam thrice. Being parallel, these connections are coplanar. In taking the transits (ab), (ac), (ad) as examples, the analytic corollary is recognized as the linear relationship of the transit times given by the second of the equalities (11).* The V_i-equations which one could set up after the pattern of the systems (14) or (16) are therefore underdetermined and the four triads must be dismissed as unfit to deliver results.

---

*With other such beam connections the relationship can be obtained by rearranging system (11).

The quartet of what may be called the cyclic triads, as (ab), (bc), (cd), is beset by different shortcomings, less unavoidable in character. It could be used for measurement, but not safely so when $\tau_i > 0$,* since, with the parameter values as chosen, it does not possess an admissibility area. Either restraining planes remain too far apart, or one of the path length conditions is violated.

By the solutions (23) the argument T = 0 defines winds whose lateral components are roughly parallel to the x- and y-axes. The elevation angle here stops near 14 degrees. Wishing to improve on that value by employing additional "auxiliary" triads we have to reject those four that include both (ac) and (bd) transits (running between beams parallel in top view). In examining their admissibility range one finds that at least one confidence requirement is not fulfilled for the Q_1,Q_3-pairs that correspond to the above lateral components.** This leaves us with a last group of four transit triads:***

AI	$d \leftrightarrow b$,	$d \leftrightarrow c$,	$c \leftrightarrow b$
AII	$d \leftrightarrow b$,	$d \leftrightarrow a$,	$a \leftrightarrow b$
AIII	$a \leftrightarrow c$,	$a \leftrightarrow d$,	$d \leftrightarrow c$
AIV	$a \leftrightarrow c$,	$a \leftrightarrow b$,	$b \leftrightarrow c$.

In dealing with them one will follow the same steps as were taken when studying the basic triads I, II, III, and IV. It seems excusable, then, to suppress much of the detail work which the reader, if so inclined, can supply by himself.

The solution groups associated with the four auxiliary triads emerge as

---

* Other possibilities have not been probed into.

** These ("unilateral") triads make use of only one pair of beams in alphabetical sequence. They are discussed in the next section.

*** They forgo the use of one beam each ("three-beam" triads).

$$\begin{cases} V_1 = -\dfrac{\lambda s}{1+\lambda^2}\dfrac{1}{\tau_2}(2+\lambda D) & \tau_1 \equiv \tau^*_{cb} \\ V_2 = -\dfrac{\lambda s}{1+\lambda^2}\dfrac{1}{\tau_2}(D-2\lambda) & \tau_2 \equiv \tau^*_{db} \\ V_3 = \dfrac{\lambda s}{1+\lambda^2}\dfrac{1}{\tau_2}\dfrac{T}{\sigma} & \tau_3 \equiv \tau^*_{dc}\ . \end{cases} \qquad (44AI)$$

$$\begin{cases} V_1 = -\dfrac{\lambda s}{1+\lambda^2}\dfrac{1}{\tau_2}(2+\lambda D) & \tau_1 = \tau^*_{da} \\ V_2 = -\dfrac{\lambda s}{1+\lambda^2}\dfrac{1}{\tau_2}(D-2\lambda) & \tau_2 = \tau^*_{db} \\ V_3 = -\dfrac{\lambda s}{1+\lambda^2}\dfrac{1}{\tau_2}\dfrac{T}{\sigma} & \tau_3 = \tau^*_{ab}\ . \end{cases} \qquad (44AII)$$

$$\begin{cases} V_1 = -\dfrac{\lambda s}{1+\lambda^2}\dfrac{1}{\tau_2}(2\lambda-D) & \tau_1 \equiv \tau^*_{dc} \\ V_2 = -\dfrac{\lambda s}{1+\lambda^2}\dfrac{1}{\tau_2}(2+\lambda D) & \tau_2 \equiv \tau^*_{ac} \\ V_3 = \dfrac{\lambda s}{1+\lambda^2}\dfrac{1}{\tau_2}\dfrac{T}{\sigma} & \tau_3 \equiv \tau^*_{ad} \end{cases} \qquad (44AIII)$$

$$\begin{cases} V_1 = -\dfrac{\lambda s}{1+\lambda^2}\dfrac{1}{\tau_2}(2\lambda-D) & \tau_1 \equiv \tau^*_{ab} \\ V_2 = -\dfrac{\lambda s}{1+\lambda^2}\dfrac{1}{\tau_2}(2+\lambda D) & \tau_2 \equiv \tau^*_{ac} \\ V_3 = -\dfrac{s}{1+\lambda^2}\dfrac{1}{\tau_2}\dfrac{T}{\sigma} & \tau_3 \equiv \tau^*_{bc} \end{cases} \qquad (44AIV)$$

It will be remembered that, if an eddy train moves from the beam first named in the double-letter subscripts to the one named second, the travel time is counted positive, otherwise negative. By imposing conditions on V_3 analogous to the inequalities (20) such that $|V_3|$ can become large one arrives at the conclusion that the three travel times pertinent to a given triad must either be all positive or all negative. Experimental values for them must now be arranged in four more sequences τ_1, τ_2, τ_3:

(cb), (db), (dc)

(da), (db), (ab)

(dc), (ac), (ad)

(ab), (ac), (bc).

After establishing an admissibility area for Q_1 and Q_3, one can determine whether or not one of these sequences marks a valid measurement. If so, the wind vector components can be computed from the pertaining solution group. Any sequence not exhibiting equal signs can here be eliminated at once.

In the sets (44) the symbols D and T have the former meanings (22). However, their roles are interchanged. D is now equivalent to an azimuth, while the allowable T-variation gives the elevation range at D = const., since

$$\tan \chi = \pm \frac{T \tan \psi}{\sqrt{D^2 + 4}} \,. \tag{45}$$

Owing to this interchange the operational domain of an auxiliary triad is radically different from that of a basic triad where it comprises upward horizontal and downward winds that arrive, roughly, from a certain φ-compass adjacent to one of the coordinate angle bisectors. Consider the triad AI, for example. One can show that, with admissible values of Q_1 and Q_3, the quantity T is always positive.* By contrast, D can be negative as well as positive

*Horizontal winds, incidentally, are therefore not measurable by auxiliary triads when the τ_i have equal signs. Unequal signs have been tried also. Indications are, however, that if such times are measured, no confidence can be placed in wind determination.

(and zero). Contemplation of the solutions (44AI) reveals that the triad AI is capable of monitoring upward (downward) winds arriving from forward (backward) directions provided that $\tau_2 > 0$ ($\tau_2 < 0$). Opposite winds are captured by AII-transits. The first two auxiliary triads then combine to handle eddy paths whose parallels drawn through the coordinate origin group around the x-axis. Those grouping around the y-axis are observable by the triads AIII and AIV, each of which carries half the load in a similar manner. These results are encouraging, for precisely those lateral directions are favored in which we wish to extend the elevation angle range. By contrast, the last quartet excluded in the survey of triads can be shown to favor the bisector directions.

Unified travel path and layer thickness restrictions again determine the bounds of the admissibility area. Wishing to explore them along the diameters D = const. (φ = const.), we formulate in terms of $D = Q_3 - Q_1$ and $T = Q_1 + Q_3 - 2$.

$$\begin{cases} R_1^* = \dfrac{2\lambda s}{\sqrt{1+\lambda^2}} \dfrac{\sqrt{D^2 + 4 + T^2 \tan^2\psi}}{T + 2 - D} \\[2ex] R_2^* = \dfrac{\lambda s}{\sqrt{1+\lambda^2}} \sqrt{D^2 + 4 + T^2 \tan^2\psi} \\[2ex] R_3^* = \dfrac{2\lambda s}{\sqrt{1+\lambda^2}} \dfrac{\sqrt{D^2 + 4 + T^2 \tan^2\psi}}{T + 2 + D} \end{cases} \tag{46}$$

$$\begin{cases} \delta_{12} = \dfrac{1}{2} \dfrac{\lambda h}{1+\lambda^2} \dfrac{(D^2 + 4 - T^2)(D^2 + 4 - DT)}{(T + 2 - D)(D^2 + 4)\sqrt{1 + \dfrac{T^2 \tan^2\psi}{D^2+4}}} \\[3ex] \delta_{23} = \dfrac{1}{2} \dfrac{\lambda h}{1+\lambda^2} \dfrac{(D^2 + 4 - T^2)(D^2 + 4 + DT)}{(T + 2 + D)(D^2 + 4)\sqrt{1 + \dfrac{T^2 \tan^2\psi}{D^2+4}}} \\[3ex] \delta_{31} = -\dfrac{2\lambda h}{1+\lambda^2} \dfrac{(D^2 + 4 - T^2)(D^2 + 4 + 2T)}{(D^2 + 4)[(T + 2)^2 - D^2]\sqrt{1 + \dfrac{T^2 \tan^2\psi}{D^2+4}}} \end{cases} \tag{47}$$

where, as agreed upon earlier,

$$\tan\psi = \frac{1}{2}, \qquad \frac{\lambda s}{\sqrt{1+\lambda^2}} = 22, \qquad \frac{\lambda h}{1+\lambda^2} = 11.$$

The number indices refer to the transits considered in the various triads as they are spelled out in the τ_i-definitions affixed to the solutions (44A). The formulas are applicable in all four transit groups alike, so that again one single admissibility area is relevant for all auxiliary triads.

Appraisal of the relative magnitude of the layer thicknesses $|\delta_{ik}|$ leads to the following precepts:

Rule III:

$$\text{If } D \geqq 0 \text{ and } D^2 + 4 - DT \begin{cases} > 0 \\ < 0 \end{cases} \text{ restrict } \begin{cases} \delta_{21} \\ \delta_{23} \end{cases}.$$

Rule IV:

$$\text{If } D \leqq 0 \text{ and } D^2 + 4 + DT \begin{cases} > 0 \\ < 0 \end{cases} \text{ restrict } \begin{cases} \delta_{31} \\ \delta_{12} \end{cases}.$$

The value of $|\delta_{ik}|$ at right is the largest of the three in the circumstances indicated.

It was found that, before the δ_{12}-restriction becomes operative, a path-length condition always limits the admissibility area, one-half of which is depicted on Figure 5 ($D > 0$). The other half (for $D < 0$) is symmetric to it with respect to the axis $D = 0$. One can show that in the interior the travel paths and layer thicknesses remain within the prescribed bounds. However, a small part of the area has been cut off, since, in it, the azimuth error can become uncomfortably large.

The worst possible errors are estimated in the manner adopted when dealing with the basic triads. With $D > 0$, it yields the expressions*

*Figure 5 shows that, within the admissibility area for $D > 0$, $Q_3 > 1$ always. Accordingly, the original denominator quantity τ_2 has been replaced by Q_3 everywhere.

$$\left(\frac{\Delta V}{V}\right)_{larg.} = \frac{1}{10Q_3} \frac{2|T-8| + Q_1^2|4D-T| + Q_3^2|4D+T|}{4(D^2+4) + T^2}$$

$$(\Delta\varphi)_{larg.} = \frac{1}{5Q_3} \frac{|Q_3-Q_1| + Q_1^2 + Q_3^2}{D^2+4}$$

$$(\Delta\chi)_{larg.} = \frac{1}{5Q_3} \frac{2[D^2 + 2(T+2)] + Q_1^2|D^2+4+TD| + Q_3^2|D^2+4-TD|}{\sqrt{D^2+4}\,[4(D^2+4) + T^2]} .$$

It is readily seen that, when Q_1 and Q_3 exchange roles, as they do with $D < 0$, the error estimates remain numerically unaffected.

On $D = 0$ the worst foreseeable azimuthal error appears as

$$(\Delta\varphi)_{larg.} = Q_3/10,$$

and, if it is to be limited to 15°,* requires that Q_3 must not grow beyond 2.618. In a like manner, the admissibility area is to be cut back for other small values of D (< 0.4).

The worst strength error estimates range between 7 and 12 percent. The χ-errors remain below 7 degrees and can be as little as 1 degree. These figures appear acceptable.

With positive values of D and τ_2 the auxiliary triad AI monitors upward winds blowing into the first quadrant from azimuths not too large.** Expression (45) here applies with the positive sign, so that, at a fixed azimuth D, the positive angle χ increases with T. On Figure 5 it grows from the lower boundary to the upper boundary when one follows a line D = const. For some of these lines, the lowest and largest values are listed in the table below. The right half-columns give the corresponding values at the same azimuths*** when the basic triads I and III are operative. They are taken from Tables I and III.

---

* In reference 1, $\Delta\varphi$ = 16 degrees was considered tolerable.

** $V_1 = 0$ obviously cannot be obtained with $D > 0$, $\tau_2 > 0$.

*** By the sets (44AI) and (23I) an azimuth described in AI by D = c is given by T = c in I. The value c = -0.2 is included, since it also can be handled by the triads. It designates a wind blowing into the fourth quadrant at a negative azimuth of small magnitude.

TABLE IV

Elevation Angle Ranges Measurable by Triads AI, I, and III

D	-0.2		0		0.2		0.5		1	
$\check{\chi}°$	7.2	0	7.6	0	7.2	0	9.1	0	11.9	0
$\hat{\chi}°$	40.2	6.8	39.0	14	40.2	21.5	38.9	24.2	32.1	32.6

D	1.5		2		3		4		5	
$\check{\chi}°$	14.6	0	16.7	0	19.5	0	21.1	10.9	23.5	15.7
$\hat{\chi}°$	29.4	33.7	28.6	33.8	29.9	34.0	32.1	33.7	33.6	33.2

While the three-beam triad is not suitable for detecting horizontal winds ($\check{\chi} = 0°$), its use quite conspicuously enlarges the top elevation accessible near D = 0 ($\varphi \approx 0$).

Table IV in essence is valid for any pair of triads intended to work on (more or less) the same winds. Inconsequential sign inversions may become necessary, a trivial case being that of downward winds ($\chi < 0$), when, for example, triads AII and I are combined. Triads AI and IV operate on upward winds arriving from the left front side. Here, $D < 0$ in the set (44AI), so that in Table IV the head row must be given inverted signs.* This is also necessary when combining triads AIII and II whose common targets are upward winds blowing into the first quadrant at azimuths not too small. D = 0 here corresponds to a wind with

$$\varphi = \text{arc tan}\ \frac{1}{\lambda}$$

(close to 90° when λ is sufficiently small). Triad II can handle such winds between 0 and $\approx$ 14 degrees elevation angles, while AIII extends the range up to at least 39 degrees.

---

*D = -c then corresponds to T = c in expressions (23IV), where τ_2 has to be negative; otherwise, IV would monitor winds from the right back side.

Analogous correspondences hold with any other pertinent combination of auxiliary and basic triads: The three-beam triads do provide the service expected of them. Horizontal winds, for which they are useless, are handled by the basic triads.*

X. CONTROLLING TRIADS

The striking similarity of the solution groups associated with the basic and the A-triads seems to be bound up with their common use of two sequential transits. Deviating forms were found when dealing with the "cyclic" triads (three sequential transits) and the "unilateral" triads (one transit only between beams in alphabetical sequence). The latter constitutes a useable second group of auxiliaries. Although it does not extend the range of safely measurable wind vectors, it may be utilized to check results ("controlling" triads). Adding another set does not appreciably increase the evaluation burden, since the main part of it, namely the back-and-forth correlation of the six record pairs, must be carried out in any event. After including this group twelve of the sixteen meaningful combinations of three transits each have been put to work.

The V_i solutions related to the controlling auxiliaries exhibit a pecularity which ought to be rooted in features of the beam geometry that are hidden in the formulas (7) so far used to obtain solution systems in a routine manner. To bring them out we note at first that any two beams, m and n, are contained in two parallel planes whose common normal ("binormal") is in the direction of the vector

$$\underline{N}_{mn} = \underline{\mu} \times \underline{\nu}$$

where the coefficients μ_i and ν_i are the direction cosines of the beams m and n, respectively.

Of the parallel eddy trains carried along by a wind of uniform velocity $\underline{V}$ a single one, as we know, is capable to connect the beams m and n. The terminal points of the connecting line are given by the position vectors (6) which have the general form

*With a carefully contrived different arrangement of three beams, such winds can be measured, although in a limited range of azimuths only (reference 1).

$$\underline{r}^*_{mn} = \underline{r}_m + \underline{\mu} F$$

$$\underline{r}^*_{nm} = \underline{r}_n + \underline{\nu} G.$$

An eddy moving from m to n will cover the distance

$$\Delta\underline{r}^* = \underline{r}^*_{nm} - \underline{r}^*_{mn}$$

whose direction is parallel to the wind (i.e., the time τ^*_{mn} needed for the movement is positive). The projection of the movement onto the binormal, namely,

$$\underline{V} \cdot \frac{\underline{N}_{mn}}{|\underline{N}_{mn}|}$$

requires the same time to cover the projected distance

$$\Delta\underline{r}^* \cdot \frac{\underline{N}_{mn}}{|\underline{N}_{mn}|} ,$$

so that the relation exists

$$\frac{1}{\tau^*_{mn}} (\underline{r}_n - \underline{r}_m) \cdot \underline{N}_{mn} = \underline{V} \cdot \underline{N}_{mn} \qquad (48)$$

where the above expressions for $\underline{r}^*_{mn}$ and $\underline{r}^*_{nm}$ were inserted into the original triple scalar product

$$(\underline{r}^*_{nm} - \underline{r}^*_{mn}) \cdot \underline{N}_{mn}$$

to obtain the simplified version at left.

This derivation of a direct equation* for the velocity components is mainly given here to emphasize the dominant role of the binormal.

Winds blowing into the first quadrant will in general move from a to c, from d to b (τ^*_{ac}, τ^*_{db} will be positive). The binormal expressions associated with these beam pairs,

$$\underline{N}_{ac} = 2\sigma\alpha_3 (\lambda\underline{i} + \underline{j}),$$

$$\underline{N}_{db} = 2\sigma\alpha_3 (\underline{i} - \lambda\underline{j}),$$

define vectors of equal length which are orthogonal to each other and parallel to the ground plane.

The third of these peculiar properties causes the right side of equation (48) to lose the component V_3 (its coefficient becoming zero). As a curious consequence, the components V_1 and V_2 are determined by the (ac)- and (db)-transits alone. They suffice for measuring the horizontal wind component; however, as will be seen shortly, admissibility criteria limit the φ-range and prevent the observation of winds purely horizontal.

Adding to the (ac), (db) transits, first the (ab)-connection, secondly the (dc)-connection, in order to compute the CI- CII-groups, we arrive at the solution systems

$$\begin{cases} V_1 = -\dfrac{2\lambda s}{1+\lambda^2}\dfrac{1}{\tau_2}(\lambda Q_1 + Q_3) & \tau_1 \equiv \tau^*_{ac} \\ V_2 = -\dfrac{2\lambda s}{1+\lambda^2}\dfrac{1}{\tau_2}(Q_1 - \lambda Q_3) & \tau_2 \equiv \tau^*_{ab} \\ \sigma V_3 = -\dfrac{2\lambda s}{1+\lambda^2}\dfrac{1}{\tau_2}(1 - Q_1 - Q_3) & \tau_3 = \tau^*_{db} \end{cases} \tag{49CI}$$

---

*It was used to write down the set (12) in reference 1.

$$\begin{cases} V_1 = -\dfrac{2\lambda s}{1+\lambda^2}\dfrac{1}{\tau_2}(\lambda Q_1 + Q_3) & \tau_1 \equiv \tau^*_{ac} \\ V_2 = -\dfrac{2\lambda s}{1+\lambda^2}\dfrac{1}{\tau_2}(Q_1 - \lambda Q_3) & \tau_2 \equiv \tau^*_{dc} \\ \sigma V_3 = -\dfrac{2\lambda s}{1+\lambda^2}\dfrac{1}{\tau_2}(Q_1 + Q_3 - 1) & \tau_3 \equiv \tau^*_{db}. \end{cases} \qquad (49CII)$$

Since with both systems

$$\tan\varphi = \frac{Q_1 - \lambda Q_3}{\lambda Q_1 + Q_3},$$

the admissible φ-ranges not only overlap, but are altogether congruent. The triads thus duplicate the measurement of winds blowing into the first ($\tau_i > 0$) or into the third ($\tau_i < 0$) quadrants. Record evaluation has to look for either three positive or three negative transit times. The ratio Q_1 and Q_3 are positive.

For winds arriving in the fourth and second quadrants, suitable transit combinations are

CIII	$d \longleftrightarrow b$,	$c \longleftrightarrow b$,	$c \longleftrightarrow a$
CIV	$d \longleftrightarrow b$,	$d \longleftrightarrow a$,	$c \longleftrightarrow a$.

They give rise to the solution systems

$$\begin{cases} V_1 = \dfrac{2\lambda s}{1+\lambda^2}\dfrac{1}{\tau_2}(\lambda Q_3 - Q_1) & \tau_1 \equiv \tau^*_{db} \\ V_2 = \dfrac{2\lambda s}{1+\lambda^2}\dfrac{1}{\tau_2}(Q_3 + \lambda Q_1) & \tau_2 \equiv \tau^*_{cb} \\ \sigma V_3 = \dfrac{2\lambda s}{1+\lambda^2}\dfrac{1}{\tau_2}(1 - Q_1 - Q_3) & \tau_3 \equiv \tau^*_{ca} \end{cases} \qquad (49CIII)$$

$$V_1 = \frac{2\lambda s}{1+\lambda^2}\frac{1}{\tau_2}(\lambda Q_3 - Q_1) \qquad \tau_1 = \tau^*_{db}$$

$$V_2 = \frac{2\lambda s}{1+\lambda^2}\frac{1}{\tau_2}(Q_3 + \lambda Q_1) \qquad \tau_2 = \tau^*_{da} \qquad (49CIV)$$

$$V_3 = \frac{2\lambda s}{1+\lambda^2}\frac{1}{\tau_2}(Q_1 + Q_3 - 1) \qquad \tau_3 = \tau^*_{ca}$$

These triads minister to winds directed toward the fourth quadrant (if $\tau_i > 0$), and toward the second quadrant (if $\tau_i < 0$). They both measure the same wind, if it is measurable at all.

For calculating the confines of the admissibility area we need the path length and layer thickness expressions which again can be unified and are valid for all four triads alike:

$$R^*_i = \frac{2\lambda s}{\sqrt{1+\lambda^2}}\frac{\sqrt{(Q_1^2 + Q_3^2) + (1 - Q_1 - Q_3)^2 \tan^2\psi}}{Q_i}, \qquad Q_2 = 1,\ i = 1,2,3 \qquad (50)$$

$$\left\{\begin{aligned}
\delta_{12} &= \frac{\lambda h}{1+\lambda^2}\frac{(2Q_1 + 2Q_3 - 1 - 2Q_1Q_3)(Q_1Q_3 - Q_1^2 - Q_3)}{Q_1(Q_1^2 + Q_3^2)\sqrt{1 + \frac{(1-Q_1-Q_3)^2}{Q_1^2 + Q_3^2}\tan^2\psi}} \\
\delta_{23} &= \frac{\lambda h}{1+\lambda^2}\frac{(2Q_1 + 2Q_3 - 1 - 2Q_1Q_3)(Q_1Q_3 - Q_3^2 - Q_1)}{Q_3(Q_1^2 + Q_3^2)\sqrt{1 + \frac{(1-Q_1-Q_3)^2}{Q_1^2 + Q_3^2}\tan^2\psi}} \\
\delta_{31} &= \frac{\lambda h}{1+\lambda^2}\frac{2Q_1 + 2Q_3 - 1 - 2Q_1Q_3}{Q_1Q_3\sqrt{1 + \frac{(1-Q_1-Q_3)^2}{Q_1^2 + Q_3^2}\tan^2\psi}},
\end{aligned}\right. \qquad (51)$$

where

$$\tan\psi, \quad \frac{\lambda s}{\sqrt{1+\lambda^2}}, \quad \frac{\lambda h}{1+\lambda^2}$$

have the numerical values adopted earlier. Assisted by the fact that Q_1 and Q_3 are positive one demonstrates that, of these three distances,

$$\begin{cases} |\delta_{12}| \text{ is largest if } Q_3 - Q_1 < - \frac{Q_1}{Q_3}, \\ |\delta_{23}| \text{ is largest if } Q_3 - Q_1 > \frac{Q_3}{Q_1} \\ |\delta_{31}| \text{ is largest if } - \frac{Q_1}{Q_3} < Q_3 - Q_1 < \frac{Q_3}{Q_1}. \end{cases} \tag{52}$$

As an application consider the case $V_3 = 0$ ($Q_1 + Q_3 = 1$) where

$$\delta_{31} = \frac{\lambda h}{1+\lambda^2} \frac{1 - 2Q_1 + 2Q_1^2}{Q_1(1 - Q_1)}$$

must be restricted. This function's minimum at $Q_1 = 1/2$ tells that

$$\delta_{31} \geqq 22.$$

The two restraining planes thus are always too far apart by our standards. Horizontal winds cannot be measured with confidence. As a consequence, the admissibility area (Figure 6) separates into two parts, the upper and larger one valid for $Q_1 + Q_3 > 1$, the other one for $Q_1 + Q_3 < 1$.

An error analysis was carried out following the earlier pattern. The worst errors likely to be encountered in the admissibility regions were estimated as ≈ 12 percent in speed, ≈ 6 degrees in azimuth, ≈ 8 degrees in elevation angle. The latter relatively large value was found more or less throughout the realm $Q_1 + Q_3 < 1$ (lower area), while in the upper area $\Delta\chi$ ran up to at most ≈ 4.5 degrees, which value is more in line with the maximum obtained for the basic triads.* Conversely, the speed and azimuth error estimates attain their larger values in the upper area, especially along the line $Q_1 = Q_3$.**

---

* $\Delta\chi = 7$ degrees was tolerated with the A-triads.

** This line again divides the areas into two symmetric halves.

The χ-ranges safely measurable, regrettably, are not wider than those amenable through the basic and A-triads. As before, they are different with wind azimuth. For comparison we note that an azimuth described by T when using triad I is associated with

$$2\,\frac{Q_1}{Q_3} = T$$

when using CI or CII. On Figure 6, therefore, a given azimuth resides along the lines

$$\frac{Q_1}{Q_3} = \frac{T}{2} = \text{const.}$$

which, when cutting through the admissibility area, define the terminal values of the χ-range as those pertaining to their points of intersection with the area boundaries. For this reason, there are two different upper values depending on whether V_3 is larger or smaller than zero. The two lower values, however, were found to coincide (as can be shown they must). In Table V, CI and CII-transits are considered for azimuths which are also monitored by triad I transits. It is representative as well for the ranges that can be attained with winds arriving from the other lateral directions.

TABLE V

Elevation Angle Ranges Measurable by Triads CI and CII

T	1	1.5	2	3	4	5	6
χ°	17.4	14.8	14.0	15.5	17.4	18.9	20.1
$\hat{\chi}$ $V_3 > 0$	27.0	28.3	28.6	28.0	27.0	26.1	25.4
$\hat{\chi}$ $V_3 < 0$	32.2	29.3	28.6	29.9	32.2	32.3	25.4

Comparison with Table IV (where the entry D is equivalent to the entry

$$T\left(= 2\,\frac{\theta_1}{\theta_3}\right)$$

in Table V) shows that no improvement of the upper bounds has been achieved. Moreover, the lower bounds are all larger than those found with AI-transits.

Almost the entire admissibility area is enclosed between the lines

$$\frac{Q_1}{Q_3} = 3 \quad \text{and} \quad \frac{Q_1}{Q_3} = \frac{1}{3} .$$

By both the sets (49CI) and (49CII)

$$\tan \varphi = \frac{\frac{Q_1}{Q_3} - \lambda}{\lambda \frac{Q_1}{Q_3} + 1} .$$

Since the function at right increases with Q_1/Q_3, the permissible φ-variation runs from a value something smaller than 17 degrees to a value smaller than 72 degrees. (Analogous results apply regarding the three other quadrants).

On the whole, the C-group is thus less effective than the two others, but it can serve as a checking group for winds within specified X- and φ-ranges. To evaluate it seems advisable when such winds have been shown present through basic or A-triads.

Some eddy tracks, among them horizontal ones with $\varphi \approx 0$ (180°) or $\varphi \approx 90°$ (270°) azimuths, remain accessible through one solitary triad only. However, double and multiple observations are feasible of many wind vectors. As a striking example, take

$$\tau^*_{ab} = -2, \quad \tau^*_{bc} = 6, \quad \tau^*_{cd} = -6, \quad \tau^*_{da} = -1.2,$$

$$\tau^*_{ac} = 6, \quad \tau^*_{bd} = 3.$$

These six times describe all transits realizable in a four-beam configuration and satisfy the symmetry relations (11) as they must do theoretically. The double-letter and number indices correlations lead to the values of Q_1 and Q_3 pertinent to the several triads*; they are found admissible with not less than seven of them:

---

*Sometimes one is to recall that $\tau^*_{nm} = -\tau^*_{mn}$.

I and II (supplementary area)

III and IV (main area including horizontal wind points)

AIII

CIII and CIV.

If, in an ideal case, the six values were actually observed, they would seven times yield the same solutions:

$$V_1 = \frac{1}{3}\frac{\lambda s}{1+\lambda^2}(2 - \lambda)$$

$$V_2 = -\frac{1}{3}\frac{\lambda s}{1+\lambda^2}(1 + 2\lambda) \qquad (53)$$

$$V_3 = \frac{1}{\sigma}\frac{2}{3}\frac{\lambda s}{1+\lambda^2} = \frac{2}{3}\frac{\lambda h}{1+\lambda^2}.$$

This wind is directed toward the second quadrant with an azimuth defined by

$$\tan\varphi = -\frac{1 + 2\lambda}{2-\lambda} < -\frac{1}{2} \qquad (\varphi < 153°).$$

Its elevation is

$$\tan\chi = \frac{1}{\sqrt{5}} \qquad (\chi \approx 24.1°).$$

As follows from the position vectors (6) computed with solutions (53), all connection terminals are above ground in the present instance. It might happen on occasion that one or two are not. Such an eddy track, though geometrically existing, is physically incomplete; no transit time will be registered. However, multiple observation may yet provide a triad through which the measurement can be made.

XI. REFERENCE HEIGHT. HOMOLOGOUS BEAM SYSTEMS

Selection of the height h determines the value of λ (by the first of the formulas (37)) and that of s (by formula (39)). It completes the specifications for the beam configuration and, for any $\underline{V}$ measured, finally permits us to say, by the tips of the position vectors (6), where the observed wind had been blowing.

The need for overlapping φ-ranges of horizontal winds dictates a lower h-threshold. The upper bound (35) on λ would place it at $h \approx 47$ m, but need not be upheld any more. As far as was known at the time of its introduction, the azimuth range of horizontal winds detectable by triad I transits began at a value slightly below 0° and had to extend to 45° to secure overlapping with the analogous φ-range of triad II. Based in part on this conception, definite figures were eventually reached for the parameters essential in computing the admissibility area which display a considerably wider interval of T-values admissible at D = 0 than at the outset could have been known to exist. It runs from T = -0.529 to T = 3.438 (Tables I and II). Trial calculations revealed that, in virtue of that broad range, the original limit $\lambda = 1$ can be restored without creating gaps between succeeding φ-sectors. The necessary T- and φ-relations follow from the solutions (23).* If, e.g., we choose $\lambda = 0.6$, the φ-ranges for admissible horizontal winds are

with triad I:	-45.8° ... 26.5°
with triad II:	-0.8° ... 73.9°
with triad III:	44.2° ... 116.5°
with triad IV:	89.2° ... 163.9°.

Overlapping takes place over sectors embracing somewhat less than 30°. The entire φ-range covered is 209.7°, well above the figure of 180° that is required to measure horizontal winds around the rose. The range allotted to a single triad is more than 70°, a sweep considerably larger than the 45°-compass originally envisaged.

Taking $\lambda = 0.6$ implies that one wishes to measure near the reference height

$$h = 11 \frac{1+\lambda^2}{\lambda} = 24.9 \text{ m}.$$

*Two of them have been quoted as the formulas (30) and (31).

The parameter value (39) yields the detector distance from the origin,

$$s = 22 \frac{\sqrt{1+\lambda^2}}{\lambda} = 42.7 \text{ m.}$$

The beam direction cosines are given by the system (2) where cotg $\psi = 2$ and, from formulas (13),

$$\sigma = \frac{2}{\sqrt{1+\lambda^2}} = \frac{s}{h} = 1.715.$$

The beam arrangement can then be set out.

The smallest, not really attainable observation height ($\lambda = 1$) is $h = 22$ m. If one intends to measure below it, the basic figure 11 for the parameter combination (37) must be lowered entailing a change in the admissibility areas which must be computed guided by the same view points as before ("homologous" areas). If one keeps the maximum path length $\hat{R}$ at 154 m, the elevation angle ψ will also be different.

Relation (28) simplifies into

$$s = \frac{h}{\sqrt{1+\lambda^2}} \text{ cotg } \psi. \tag{54}$$

For practical reasons one would not wish the distance s to grow too large, so that h is also subjected to some upper threshold. With the present configuration, if $\lambda = 0.1$, $h \approx 110$ m, $s \approx 220$ m. Furthermore, the value of λ could not be lowered indefinitely lest the beams, actually of finite width, intersect in their outer fringes and thus impair the soundness of the measurement. To check into this question, consider that, by relation (54), the half diagonal length of the square aloft is

$$\lambda s \approx \lambda h \text{ cotg } \psi$$

meaning that its side is of order $2\lambda h$, or 22 m in our case, quite irrespective of observation height. The danger for the cross sections of the (slightly conical) beams to become as wide as that will probably not be encountered till one reaches into rather large heights indeed. Perhaps it can be abated yet by improving on the optical arrangement.*

In some measure the length s can be held down by decreasing cotg ψ which can be accomplished both by raising $\hat{R}$ and the limit for the δ. Let us turn matters around, starting out with demanding that cotg ψ = $\sqrt{2}$** be substituted for cotg $\psi = 2$. If in addition we acknowledge $\hat{R} = 180$ m (for 154 m) as the largest admissible path length, equation (33) yields the value

$$\frac{\lambda h}{1+\lambda^2} = 14.05.$$

Expression (36) describes the variation of the cross distance δ_{12} along $D = 0$, i.e., when horizontal winds are present. If we retain 16 m as its upper limit, we find that, when $\lambda = 0.03$, T may move between the values -0.22 and 2.5 which, with the triad I azimuths (30), correspond to $\varphi_I = -8°$ and $\varphi_I = 49.6°$. Since the sectors amenable to the three remaining triads are probably of similar width (57.6°), one can hope that the four together cover (at least) half of the rose without gap. If actual computation shows that this is not so, one would have to raise the limit on δ_{12}, because this widens the T-range, and consequently the φ-ranges of horizontal winds.

With $\lambda = 0.03$,

$$h = \frac{14.05}{0.03} = 468 \text{ m},$$

$$s = h \text{ cotg } \psi = 468\sqrt{2} = 662 \text{ m}.$$

With $\lambda = 0.03$ and the former value, cotg $\psi = 2$,

$$h = \frac{11}{0.03} = 367 \text{ m}, \qquad s = 2h = 734 \text{ m}.$$

---

* A long sleeve or tube pulled over an objective, for example, is cutting out some of the side light.

**This is the smallest value still making it reasonably certain that the minimum of the path R_3^* is encountered on the curve $\hat{R}_1^* = R$. Were it otherwise, the validity of equation (33) should be questioned.

The improvement is evident.* The admissibility area and error estimate computations can employ the text relations with the new inputs

$$\hat{R} = 180 \text{ m}, \quad \frac{\lambda h}{1+\lambda^2} = 14.05, \quad \text{cotg } \psi = \sqrt{2}.$$

The area on Figure 3, conceivably, will turn out narrower with this homologous system; the lesser scope of T-values on D = 0 may set the trend. The diminished magnitude of cotg ψ in general should allow higher χ-figures, although it could be that the opposite is true with basic triads when D is small.

In dealing with the original system it was preferred not to enforce a value of the beam elevation (as was done just now); instead, a way was sought which would lead to a suitable figure for cotg ψ out of the infinitely many that could be proposed. The outcome was a beam configuration that can be used with early experimentation operating at heights, say, between 25 m and 300 m.

XII. CONCLUSION

While it has been shown in the foregoing that, notwithstanding the delicate interplay of a number of competing conditions, beam systems can be worked out to answer immediate needs, the full capabilities of the square arrangement have not yet been explored. The so-called cyclic triads in particular have not been tried when Q_1 and Q_3 are of unequal signs, and the negative results obtained in this respect with auxiliary and controlling triads, while correct, may have overlooked favorable situations. After all, it seems odd that the basic triads alone should allow for such opposite signs. Furthermore, scant attention has been given to transit combinations where both Q_1 and Q_3 are negative. The little that has been done here was kept in the notes, because, as far as the study went, one of the path length or cross distance conditions was always violated.

---

*The lowest value barely attainable ($\lambda = 1$) is now h = 28.1 m (instead of 22 m). The altered beam system was geared to measure at larger heights (by upping the value acceptable for the length $\hat{R}$).

These questions, given sufficient time, can all be resolved within the framework of the present methods. Some modifications (minor or perhaps major) are foreseen when tackling two further problems also related to that of the present paper.

In the first place, winds with a strong vertical component so far escape detection. If there is a need for it in some quarters, means should be found to satisfy it. The task is tempting in itself, because apparently conventional meteorological experimentation is inadequately equipped to obtain information on the vertical component.

Secondly, detectors are available that can receive several beams simultaneously. In using them the number of transit combinations is apt to grow very large indeed, especially if there are two or more installed in the square arrangement. Also, the symmetry advantages will be more or less lost. On the other hand, one can operate simultaneously in neighboring regions, possibly even at markedly different heights, thus determining a wind profile. Whether or not omission of one single-beam detector is permissible without destroying the flexibility of the system should be among the first questions to be answered.

The long-standing proposal of measuring winds by mounting two detectors, at least one of them multiple, on an airplane flying horizontally at constant speed introduces an additional parameter and a vastly changed situation which is not purely geometric, but kinematic as well. The argument includes elements foreign to those used so far, and the problem would therefore seem to call for a fresh approach which, though heeding the same fundamental restraints, should end up with a methodological and computational scheme quite different in detail.

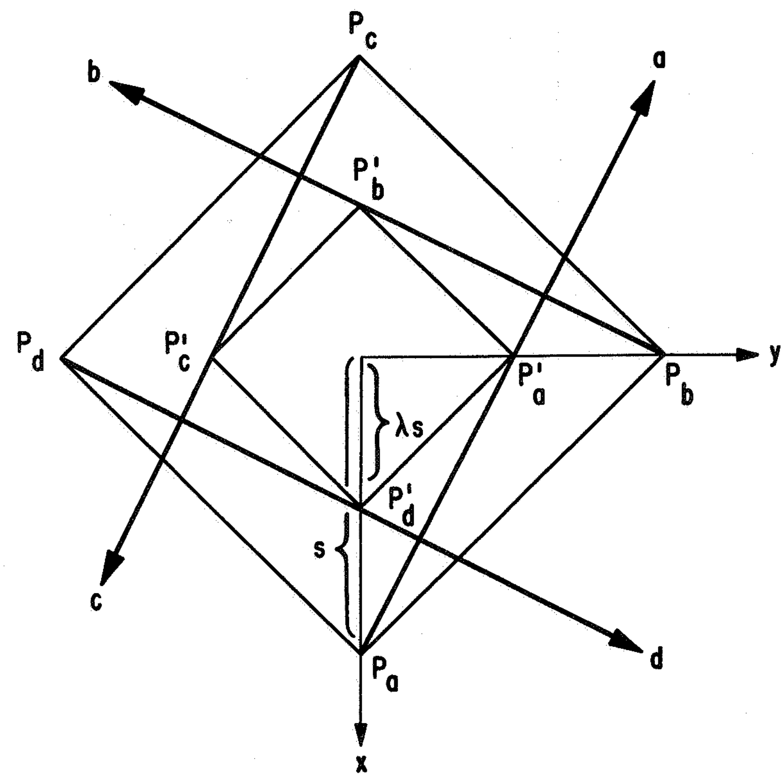

FIG. 1. TOP VIEW OF BEAM SYSTEM

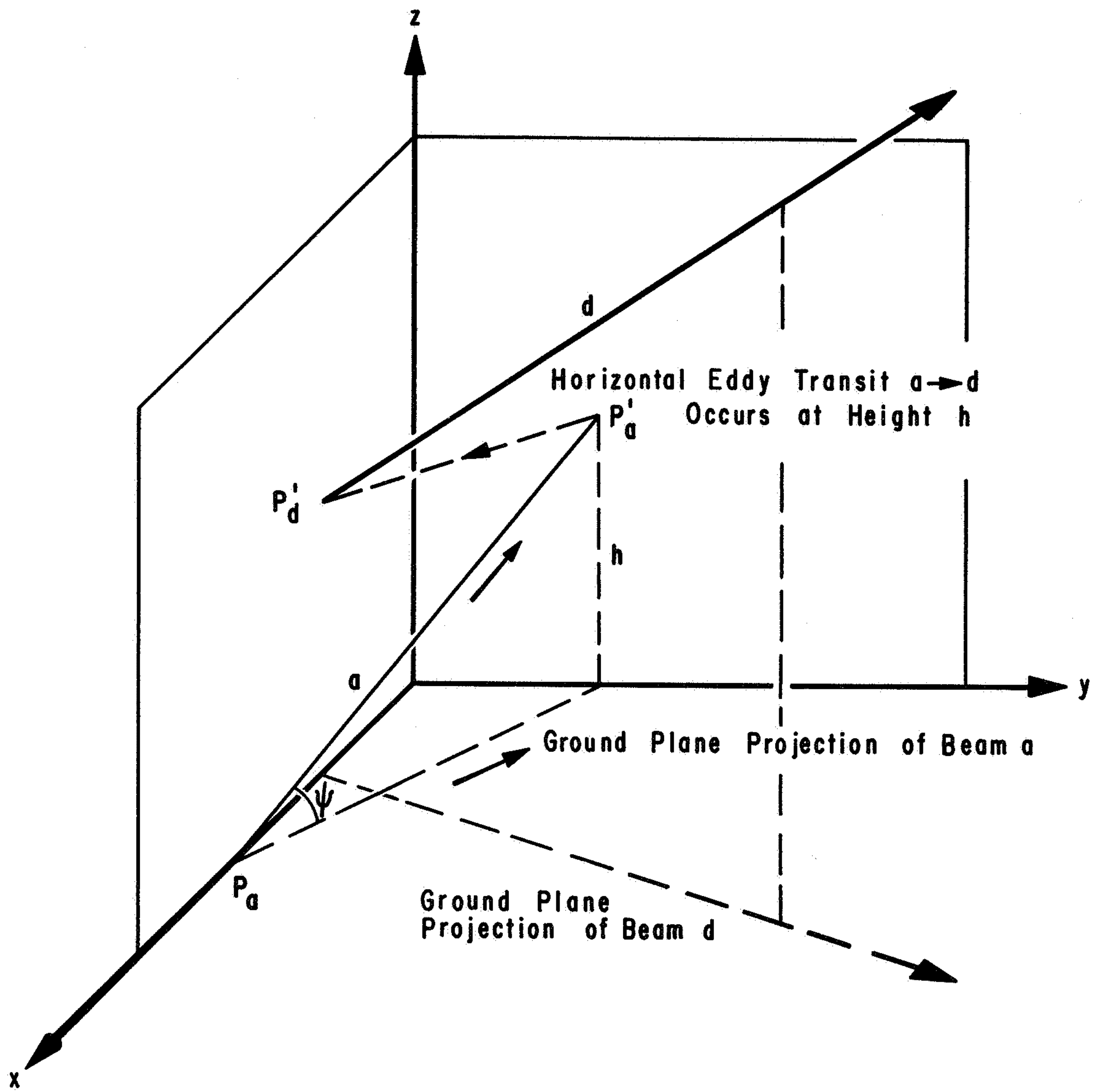

FIG. 2. BEAM CONFIGURATION IN FIRST OCTANT

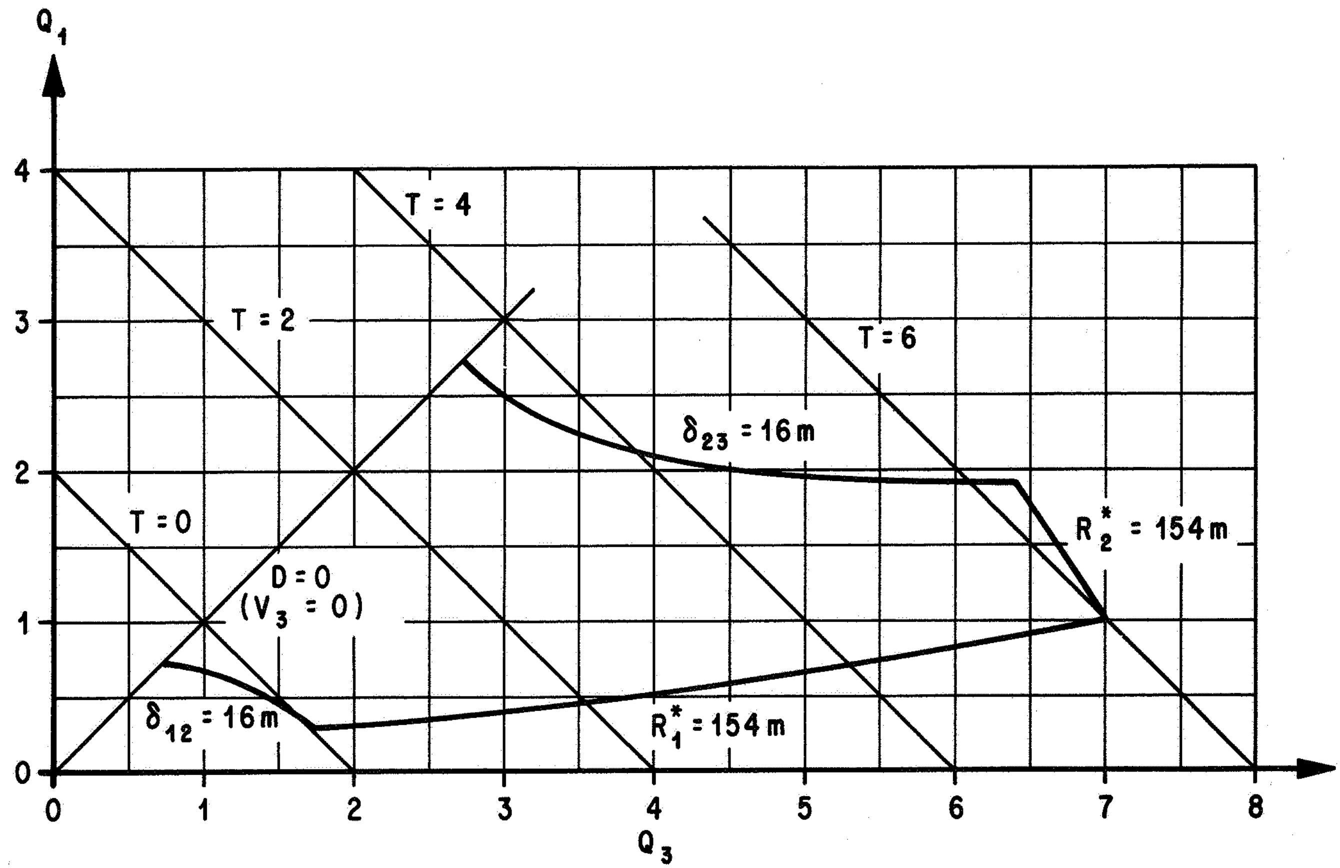

FIG. 3. ADMISSIBILITY AREA OF THE BASIC TRIADS ($V_3 \geqq 0$)

$$Q_1 = \frac{\tau_2}{\tau_1}, \quad Q_3 = \frac{\tau_2}{\tau_3}$$

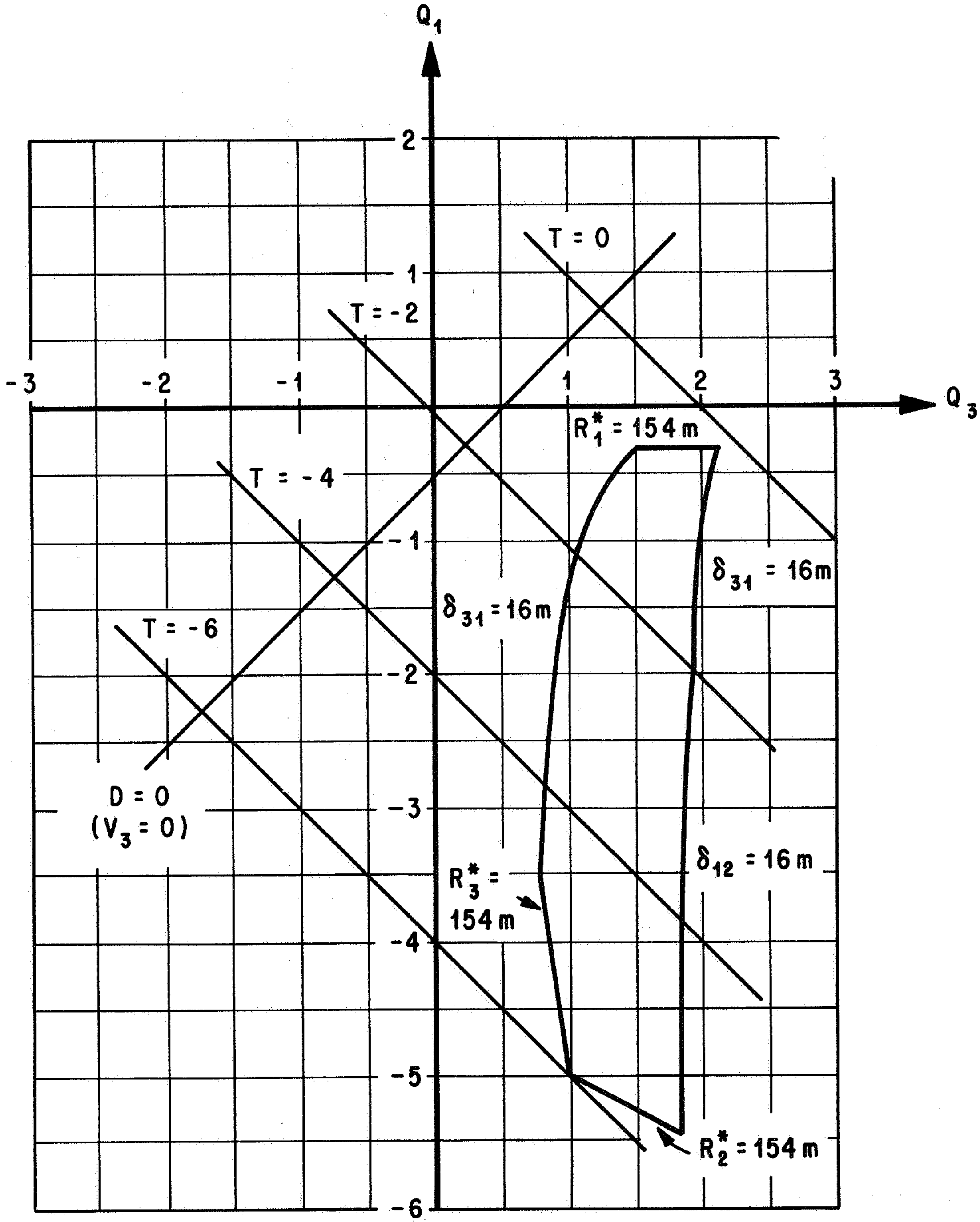

FIG. 4. SUPPLEMENTARY ADMISSIBILITY AREA OF THE BASIC TRIADS ($Q_1 < 0$, $Q_3 > 0$)

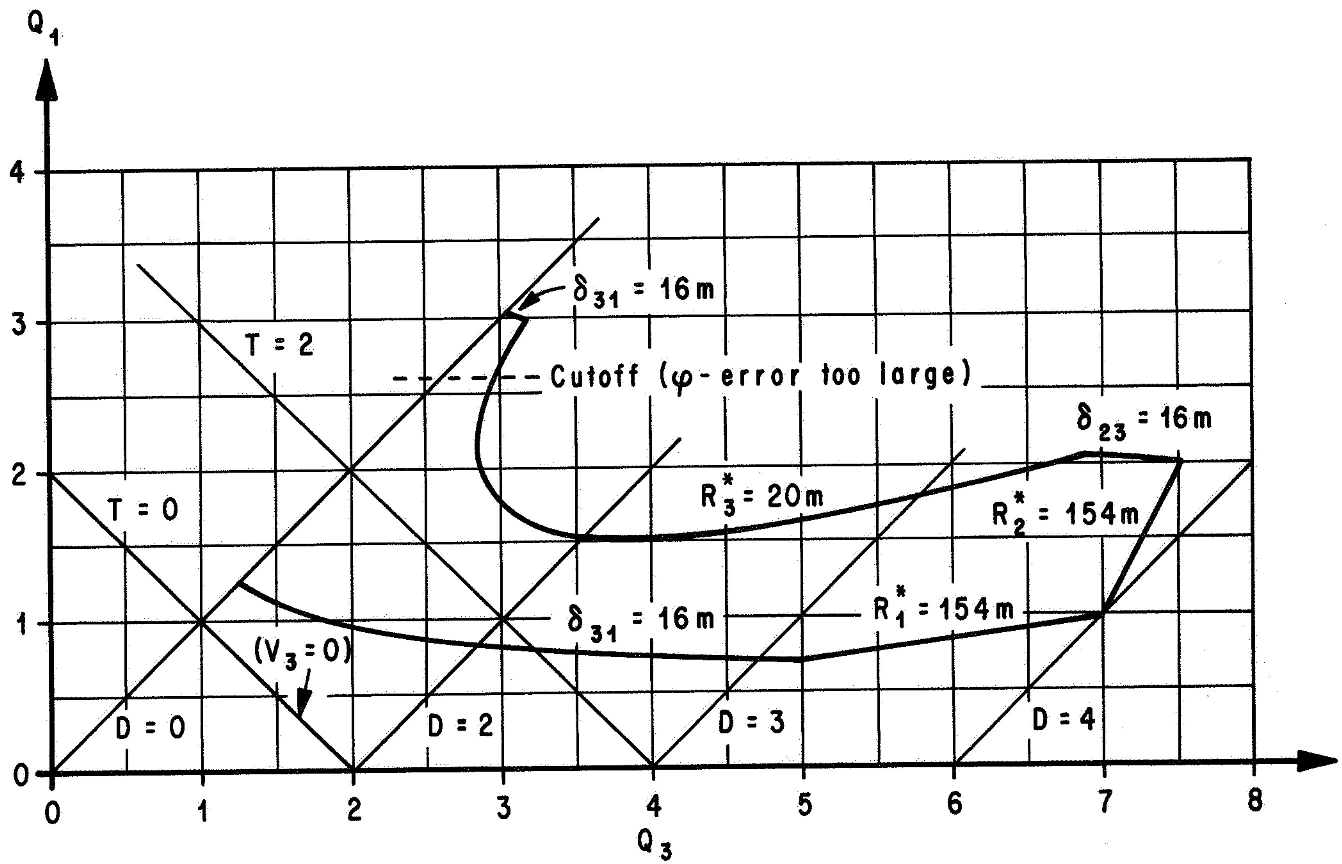

FIG. 5. ADMISSIBILITY AREA FOR AUXILIARY TRIADS

($D \geqq 0$)

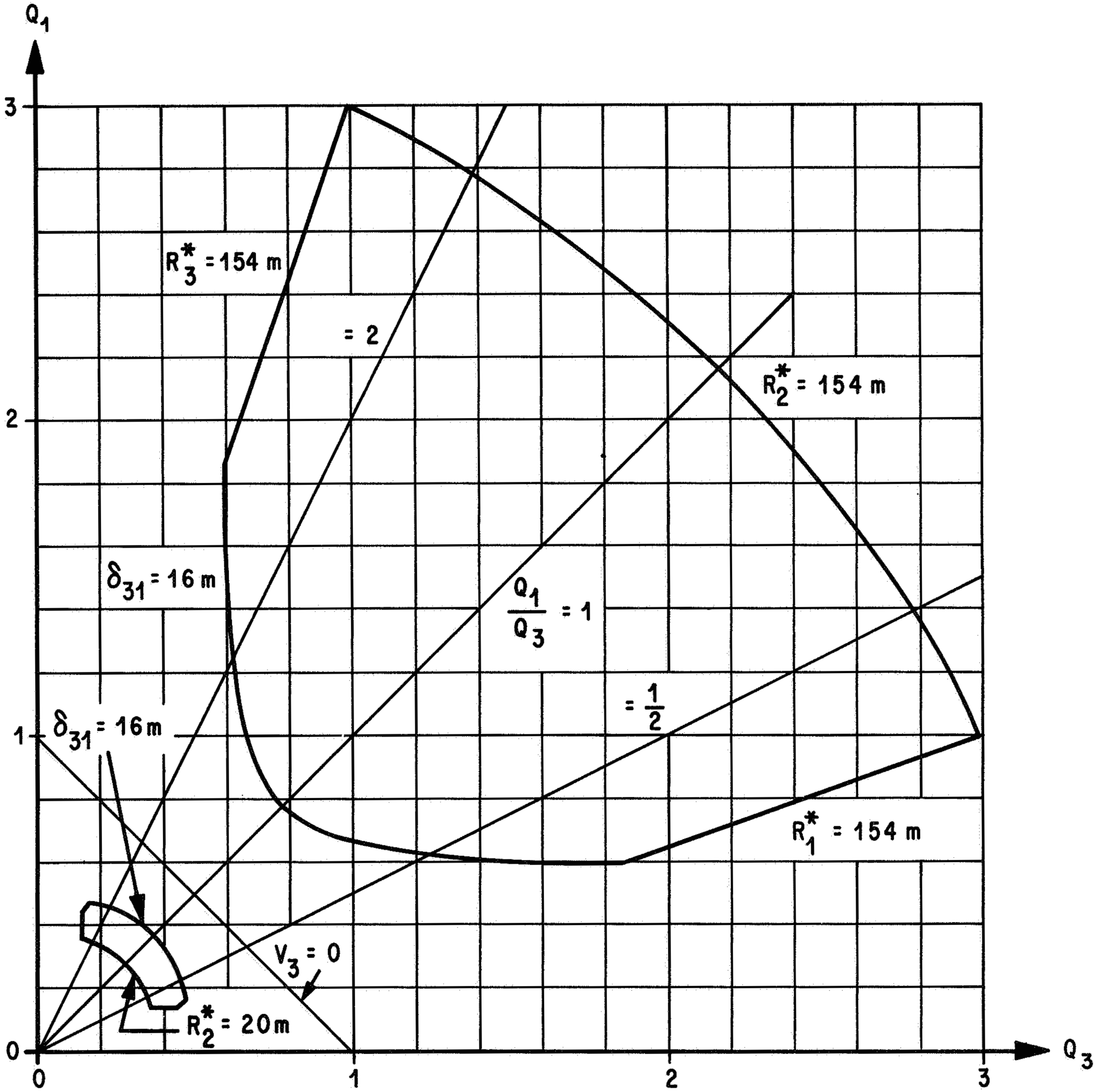

FIG. 6. TOTAL ADMISSIBILITY AREA FOR CONTROLLING TRIADS

APPROVAL NASA TM X-53982

WIND DETERMINATION BASED ON EDDY TRANSIT TIMES MEASURED BETWEEN FOUR NON-INTERSECTING LIGHT BEAMS

by W. H. Heybey

The information in this report has been reviewed for security classification. Review of any information concerning Department of Defense or Atomic Energy Commission programs has been made by the MSFC Security Classification Officer. This report, in its entirety, has been determined to be unclassified.

This document has also been reviewed and approved for technical accuracy.

E. D. Geissler
Director, Aero-Astrodynamics Laboratory

DISTRIBUTION

DIR

DEP-T
Mr. Weidner

S&E-R
Dr. Johnson
Mr. Attaya

PM-PR-M
Mr. Goldston

A&TS-PAT
A&TS-MS-H
A&TS-MS-IP
A&TS-MS-IL (8)
A&TS-TU, Mr. Wiggins (6)

S&E-AERO
Dr. Geissler
Mr. Murphree
Dr. Heybey (20)
Mr. Cummings
Dr. H. Krause
Mr. Dahm
Mr. Holderer
Mr. Reed
Mr. Heaman
Mr. Simon
Mr. Huffaker
Dr. F. Krause
Mr. Johnston
Mr. Funk
Mr. Ellner
Mr. W. Vaughan
Mr. Lindberg
Mr. I. Jones
Mr. Pickelner
Mr. Horn
Mr. Baker

Sci. & Tech. Info. Facility (25)
P. O. Box 33
College Park, Md.
Attn: NASA Rep. (S-AK/RKT)

IITRI
10 W 35th St.
Chicago, Ill.
Attn: Dr. Damkevala
Dr. Clinch
Dr. Montgomery
Dr. Wilson
Dr. Dennen
Mr. Klugman
Col. Ferrell (2)
Mr. Phillips

Nortronics
Res. Pk.
Huntsville, Alabama
Attn: Mr. Ryan (2)
Mr. Bennett
Dr. Su
Mr. Barnett
Mr. Paranjape
Mr. Cikanek
Mr. Pooley

Col. State Univ.
Ft. Collins, Colorado
Attn: Prof. Sandborn (2)

Env. Sci. Services Adm.
Boulder, Colorado
Attn: Dr. Bean (2)

Federal Aviation Agency
Washington, D. C.
Attn: Dr. Powers

NASA Headquarters
RAO, Mr. W. A. McGowan
RV-I, Mr. P. A. Cerreta
SAB, Mr. T. G. George
REI, Dr. W. A. Menzel
RV-2, Mr. D. Michel
RAA, Mr. J. Parkinson
RAP, Mr. N. Rekos
RR, Dr. Kurzweg

MSFC—RSA, Ala